Distribution of Some Minor Elements between Coexisting Sulfide Minerals [1]

GL03549

PHILIP M. BETHKE AND PAUL B. BARTON, JR.

Abstract

The distribution of cadmium, manganese and selenium between coexisting sphalerite and galena and of cadmium and manganese between wurtzite and galena has been studied experimentally over the temperature range 600°–800° C. The distribution of selenium between galena and chalcopyrite has been investigated between 390° and 595° C. Cadmium and manganese are strongly fractionated toward sphalerite or wurtzite relative to galena, while the sequence for fractionation of selenium is: galena > chalcopyrite > sphalerite. Cadmium- and manganese-bearing galena and sphalerite solid solutions appear to exhibit Henry's law behavior throughout the concentration ranges normally found in nature. Selenium-bearing galena and sphalerite solid solutions behave as sensibly ideal mixtures over the temperature range studied. Therefore, at concentration levels expected in nature distribution coefficients (K) for these systems are functions of temperature and pressure alone. Log K vs $1/T°_K$ plots are linear for each of these systems and their slope and position suggest that they may be used to estimate temperatures of ore formation to a precision of $\pm15°–20°$ C down to temperatures as low as 200° C for many deposits. The effect of pressure, as calculated from precise molar volume data, is insignificant. Values of the distribution coefficients should be determined in the range 200°–500° C to check our linear extrapolations to low temperatures. Polytyping of natural sphalerites may lead to serious underestimation of temperature if unrecognized.

The most serious barrier to the application of these data to ore deposits is the necessity for an accurate paragenetic interpretation coupled with precise sampling. The materials analyzed must represent samples that equilibrated with respect to the partitioned components at the time of deposition and that have preserved their compositions throughout the postdepositional history of the deposit. The common occurrence of growth zones suggests that in many cases it will be necessary to sample contemporaneous and internally homogeneous zones in each of the minerals. A nearly absolute degree of sample purity is required, particularly for the depleted phase. The rapid rates of solid state reaction in galena and chalcopyrite imply that both phases should be considered suspect even in low temperature environments. Concordant temperature estimates based on the partitioning of two or more elements should provide an excellent test of the degree of approach to, and preservation of, equilibrium compositions.

Introduction

THE distribution of minor elements between coexisting minerals has been suggested as a generally applicable geothermometer (Friedman, 1949; Holland, 1956; McIntire, 1963; and many others). Barton (1970) and Barton and Skinner (1967) have pointed out the advantage of using the distribution of minor elements between minerals as opposed to the minor element content of a single mineral in the estimation of the conditions of ore formation. This report describes the experimental measurement of the distribution coefficients for cadmium, manganese, and selenium between sphalerite and galena, and for selenium between galena and chalcopyrite. Our experiments show

that the distribution coefficients are independent of composition and vary sufficiently with temperature to permit reasonably precise temperature estimates. They therefore constitute a first step toward useful geothermometry. However, this method still requires extensive testing by field application, and the problems associated with such application are imposing.

We have reported our preliminary findings in abstracts (Bethke, Barton and Page, 1958, and Bethke and Barton, 1959), but additional data and more precise methods of evaluation have led to minor changes in the reported values of the distribution coefficients.

Principles

It is generally recognized that "impurity" elements may be incorporated into minerals in

several ways: in substitutional solid solution, as adsorbed films, or as components of discrete solid or fluid inclusions. In this discussion we shall consider only the solid solutions, for the surface films and extraneous phases are not amenable to quantitative interpretation and can, in theory at least, be eliminated by adequate sample preparation.

It is convenient for our purposes *not* to draw sharp distinctions between major, minor, and trace constituents. There is little difference in principle whether we consider, for instance, the distribution of sodium between plagioclase and alkali feldspar, or the distribution of manganese between sphalerite and galena. However, since most applications to ore minerals will be based on elements occurring in rather low amounts, we shall employ the term "minor component" to designate any nonessential constituent occurring in solid solution.

It is most convenient, for this discussion, to define the equilibrium distribution of a minor component between two or more phases in terms such that, at equilibrium, the *activity* of the component is the same in all phases present.[2] Let us consider, for example, the contemporaneous deposition (at equilibrium) of sphalerite and galena from an aqueous solution containing a small amount of manganese. The equilibrium statement with respect to manganese is:

$$a_{MnS}^{sp} = a_{MnS}^{gn} = a_{MnS}^{soln} \qquad (1)$$

where a_{MnS}^{sp}, and a_{MnS}^{gn}, a_{MnS}^{soln} are the activities of MnS in sphalerite, galena and the solution, respectively.[3] The mole fraction, N, of a component in solution, (either solid or aqueous) is related to its activity through the *activity coefficient*, for example:

$$N_{MnS}^{sp} = a_{MnS}^{sp}/\gamma_{MnS}^{sp} \qquad (2)$$

where N_{MnS}^{sp} and γ_{MnS}^{sp} are the mole fraction and activity coefficient of MnS in sphalerite, respectively. The activity coefficient is an inverse measure of the ability of the host phase to accommodate the minor component. Its magnitude varies with temperature, pressure and composition of the host, and may be expected to be very different in different

phases. Substituting (2) into (1) we see:

$$N_{MnS}^{sp} \cdot \gamma_{MnS}^{sp} = N_{MnS}^{gn} \cdot \gamma_{MnS}^{gn} = N_{MnS}^{soln} \cdot \gamma_{MnS}^{soln} \qquad (3)$$

and the distribution coefficient, K, defined as the ratio of the *concentrations* of the minor component in any two phases, may be written:

$$K_{MnS}^{soln-sp} = N_{MnS}^{soln}/N_{MnS}^{sp} = \gamma_{MnS}^{sp}/\gamma_{MnS}^{soln}, \qquad (4)$$

or, for the solid phases:

$$K_{MnS}^{sp-gn} = N_{MnS}^{sp}/N_{MnS}^{gn} = \gamma_{MnS}^{gn}/\gamma_{MnS}^{sp} \qquad (5)$$

Since, with the possible exception of fluid inclusions, the ore fluid is not available for analysis the partitioning between mineral pairs is the more useful situation.

We have noted that the activity coefficient, and therefore, the distribution coefficient, is, in general, a function of temperature, pressure, and composition of the host phase(s). In order to evaluate the potential usefulness of the partitioning of minor elements it is first necessary to evaluate the relative influence of each of these variables.

In general, the activity coefficient of a minor component in a solid solution varies with the concentration of the component, but as the concentration approaches zero, the activity coefficient reaches a constant value analogous to the Henry's law constant. Therefore, over the concentration range through which both minerals exhibit Henry's law behavior, the distribution coefficient will be constant. We have determined the distribution coefficients over a wide range of compositions in each of the systems studied, and with the exception of the distribution of selenium between galena and chalcopyrite, the distribution coefficient in each is sensibly constant over a compositional range many times that expected in natural assemblages.

While the activity coefficient is a function of all compositional variables in the host phase, as pointed out by Kretz (1961) and McIntire (1963), minor amounts of other components in solid solutions generally do not influence the activity coefficients of components present in low amounts to an appreciable extent.[4] An important exception is the special case of coupled substitution, e.g., $Ag^+ + Bi^{+++}$ for $2Pb^{++}$ in galena (cf. Van Hook, 1960). We have specifically chosen to work with components which do not participate in coupled substitution in the host minerals considered.

---

[2] Activity as used here is the *absolute activity* of Guggenheim (1950), $a = e^{\mu/RT}$ where μ is the chemical potential, R is the gas constant, and T is the temperature in degrees Kelvin. The absolute activity is always referred to the same standard state (such as CdS of the greenockite structure, or CdS vapor at 1 atmosphere) no matter what the nature of the phases in which the component occurs. Our definition of the distribution coefficient which follows therefore differs in *notation* from that of McIntire (1963).

[3] Although we may speak of the "manganese content" of sphalerite, we must really consider the component to be MnS not Mn because the solid solution is between ZnS and MnS not ZnS and Mn.

[4] FeS appears to be the only component commonly entering sphalerite in sufficient amounts to be of concern and most galena seems to be even less subject to such compositional influences.

The effect of temperature on the distribution coefficient may be expressed:

$$\frac{d \log K}{d(1/T)} = \frac{-\Delta \bar{H}}{2.3R} \qquad (6)$$

where $\Delta \bar{H}$ equals the difference in the partial molar enthalpies of the reactants and products of the distribution reaction (e.g., $\bar{H}_{MnS}^{sp} - \bar{H}_{MnS}^{gn}$); R is the gas constant, and T is the absolute temperature.

The effect of pressure on the distribution coefficient may be expressed:

$$\frac{d \log K}{dP} = \frac{-\Delta \bar{V}}{2.3\,RT} \qquad (7)$$

where $\Delta \bar{V}$ is the difference in the partial molar volumes of the reactants and products of the distribution reaction.

The expression for the P-T behavior of a given distribution coefficient is:

$$\frac{dT}{dP} = \frac{-T\Delta \bar{V}}{\Delta \bar{H}} \qquad (8)$$

which is one form of the Clapeyron-Clausius equation.

It should again be emphasized that the preceding discussion is predicated on the assumption of equilibrium between the coexisting pair.

Experimental Studies

As a first step in the evaluation of the potential application of the principles just discussed, several promising systems were investigated to determine if the variation of the distribution coefficient with temperature was large enough to permit reasonably precise temperature estimates, and if the magnitude of the coefficient were small enough over the presumed temperature range of ore deposition to permit precise analysis of the impoverished phase. Special attention was given to the extrapolation of our data out of the compositional range of our experiments. The results of our experiments provide a quantitative basis for the geothermometry of some natural ores.

Methods of Investigation

Our experiments consisted of determining tie-lines in the systems CdS-PbS-ZnS, MnS-PbS-ZnS, PbS-PbSe-ZnS-ZnSe and PbS-Cu$_{0.526}$Fe$_{0.526}$S-PbSe-Cu$_{0.526}$Fe$_{0.526}$Se by allowing finely powdered mechanical mixtures of the pure components or binary solid solutions to react in evacuated silica tubes at controlled temperatures. The compositions of the reaction products were determined by precise X-ray diffraction techniques. With the exception

of manganese-bearing galenas, the relationships between cell-edge and composition reported by Bethke and Barton (1961), Skinner (1961), and Skinner and Bethke (1961) were utilized as the basis for the compositional analyses.[5] The manganese content of galena was estimated by X-ray diffraction techniques on the basis of a Vegard's law assumption using values of 5.9358A and 5.2234A (Robie, Bethke and Beardsley, 1967) for the cell-edges of galena and alabandite, respectively. Because of the small solubility of MnS in galena (approximately 3.5 mole percent at 850° C) it was not considered necessary to prepare spacing-curve standards for this system. In the analogous systems reported above, any deviations from Vegard's law were too small to be detectable over this compositional range. The starting materials for this study were the same as those reported in the above papers,[6] and the end members or binary solid solutions used in compounding the runs for this study were either from the same batches or prepared in the same fashion as the compounds for which cell-edge data was reported.

The uncertainties assigned to the compositions of the reaction products are equivalent to twice the standard deviation derived in the above mentioned cell-edge versus composition studies. The uncertainty is independent of composition and at extremely low concentrations may exceed the reported concentration.

The sizes of the charges varied between 50 and 200 mg. The silica tubes were evacuated to a pressure of less than 200 microns of mercury. Temperatures of the furnaces were controlled to less than $\pm 5°$ C and were continuously recorded. The runs were quenched in cold water, and no suggestion of inadequate quench was ever noted.

Criteria for Equilibrium

The sharpness of the X-ray diffraction profiles was used as a criterion for a close approach to equilibrium. Because of the large changes in cell-edges with composition for the solid solutions

---

[5] Skinner (1961) mistakenly used weight percent instead of mole percent values for the MnS content of his four highest manganese sphalerites in his derivation of the relationship between unit cell-edge and composition of manganese-bearing sphalerites. A linear regression of Skinner's values of a_0 on his values of mole percent MnS in sphalerite, forced to pass through $a_0 = 5.4093$A for pure ZnS yields the relationship: mol % MnS $= \dfrac{a_0 - 5.4093}{0.00186}$. This recalculated relationship was used in our study.

[6] Unfortunately the analysis of the copper reagent used to prepare the chalcopyrite was omitted from our previous paper (Bethke and Barton, 1961). Baker and Adamson reagent grade copper wire was used. Semiquantitative spectrographic analysis by K. V. Hazel, of the U. S. Geological Survey, showed only the following impurities: Fe 0.001%, Mg 0.0001%, Ag 0.0003%, Ba 0.0001%, Ni 0.001%, Zn 0.03%.

involved, very slight changes in composition lead to significant angular changes in the high angle reflections used. Therefore even slight compositional heterogeneity leads to considerable broadening of the diffraction profiles. (For a relatively insensitive example, see Fig. 4 in Sims and Barton, 1961.) The formation of polytypes of sphalerite and wurtzite solid solutions was a possible source of error as it potentially affected both the distribution coefficient and the X-ray diffraction analysis. All runs containing a ZnS phase were checked for the presence of polytypes by examining low angle X-ray diffraction patterns and/or by optical methods. The runs reported herein showed no evidence of polytyping. All systems except $PbS-Cu_{0.526}Fe_{0.526}S-PbSe-Cu_{0.526}Fe_{0.526}Se$ contained runs that approached the equilibrium distribution relationship from opposite directions.

Distribution of Cadmium between Sphalerite or Wurtzite and Galena

The distribution of CdS between sphalerite or wurtzite and galena may be described in terms of the system CdS-PbS-ZnS (Fig. 1A). The system contains three crystalline phases: a CdS-bearing galena solid solution, a CdS-bearing sphalerite solid solution, and a wurtzite-greenockite solid solution. The solubility of PbS in greenockite and sphalerite is too small to bias our compositional analyses, as is the solubility of ZnS in galena. Galena will take CdS into solid solution up to approximately 25 mole percent at the eutectic temperature of about 950° C (unpublished data). Little detail is available for the ZnS-CdS binary. Wurtzite and greenockite have been shown by Hurlbut (1957) and Skinner and Bethke (1961) to be completely miscible at elevated temperatures. The sphalerite-wurtzite transition temperature

TABLE I

EXPERIMENTAL DATA IN THE SYSTEM CdS-PbS-ZnS

A. Composition of ZnS-CdS solid solutions used as starting materials in 890°C and 850°C isotherms.

Batch	Mole fraction CdS	Mole fraction ZnS
Cd101	.0207	.9793
Cd102	.0402	.9598
Cd104	.0795	.9205
Cd105	.0995	.9005
Cd106	.2956	.7044
Cd107	.4984	.5016
Cd108	.5998	.4002
Cd109	.7012	.2987
Cd110	.7980	.2019
Cd111	.8998	.1002

B. Composition, temperature, duration, and results of runs.

Run	Starting Materials	Temp. ±5°C	Time days	wz ±.002	sp ±.002	gn ±.002
	Cd101+ZnS+PbS	890°C	30		.0085	.0050
	CdS+ZnS+PbS	"	12		.0108	.0083
	Cd102+ZnS+PbS	"	30		.0146	.0064
	CdS+ZnS+PbS	"	13		.0163	.0093
	Cd104+ZnS+PbS	"	30		.0271	.0134
	CdS+ZnS+PbS	"	30		.0297	.0122
	CdS+ZnS+PbS	"	13	.0381		.0169
	Cd105+Cd101+PbS	"	30	.0389		.0162
	CdS+ZnS+PbS	"	13	.0752		.0303
	Cd106+ZnS+PbS	"	30	.1118		.0327
	CdS+ZnS+PbS	"	13	.1511		.0501
	CdS+ZnS+PbS	"	9	.1930		.0644
	Cd107+Cd105+PbS	"	30	.2478		.0609
	CdS+ZnS+PbS	"	13	.2660		.0677
	Cd108+Cd106+PbS	"	30	.3884		.0818
	Cd109+Cd107+PbS	"	30	.5378		.1016
	Cd110+Cd108+PbS	"	30	.6500		.1214
	Cd111+Cd109+PbS	"	30	.7561		.1428
	Cd110+CdS+PbS	"	30	.8731		.1648
	Cd101+ZnS+PbS	850°C	90		.0089	.0039
	Cd102+ZnS+PbS	"	90		.0156	.0057
	Cd104+ZnS+PbS	"	90		.0292	.0123
	Cd105+Cd101+PbS	"	90	.0453		.0142
	Cd106+ZnS+PbS	"	90	.1162		.0274
	Cd107+Cd105+PbS	"	90	.2520		.0501
	Cd108+Cd106+PbS	"	90	.4220		.0710
	Cd109+Cd107+PbS	"	90	.5570		.0844
	Cd110+Cd108+PbS	"	90	.6568		.1018
	Cd111+Cd109+PbS	"	90	.7606		.1209
	Cd110+CdS+PbS	"	90	.8798		.1395

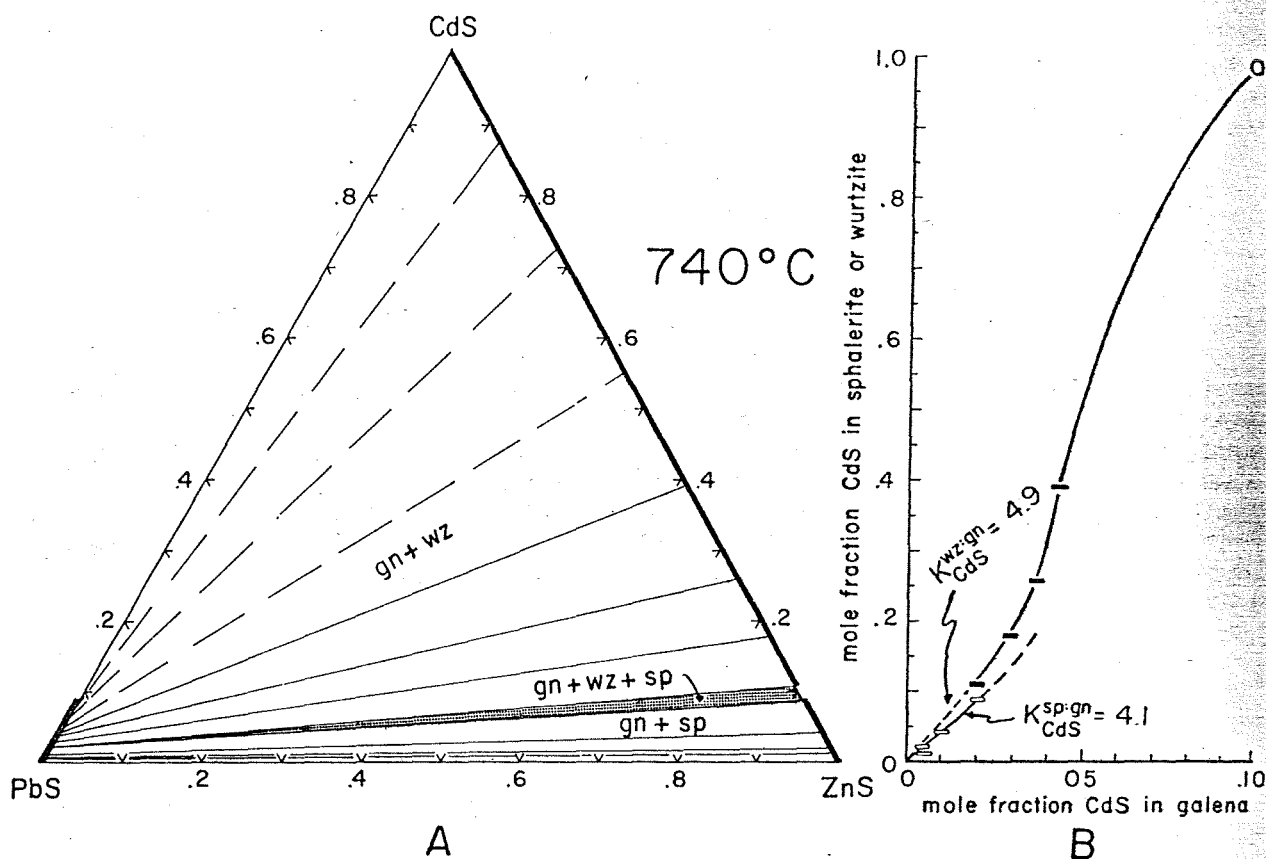| Run	Starting Materials	Temp. ±5°C	Time days	wz ±.002	sp ±.002	gn ±.002
Cd27B	CdS+ZnS+PbS	820°C	15		.0132	.0062
Cd26B	CdS+ZnS+PbS	"	15		.0208	.0067
Cd25B	CdS+ZnS+PbS	"	15		.0375	.0134
Cd24B	CdS+ZnS+PbS	"	15	.0935		.0235
Cd23B	CdS+ZnS+PbS	"	15	.1869		.0389
Cd21B	CdS+ZnS+PbS	"	15	.2625		.0508
Cd22B	CdS+ZnS+PbS	"	15	.3585		.0556
Cd27C	CdS+ZnS+PbS	740°C	21		.0134	.0048
Cd26C	CdS+ZnS+PbS	"	21		.0200	.0043
Cd25C	CdS+ZnS+PbS	"	21		.0404	.0100
Cd24C	CdS+ZnS+PbS	"	21	.1069	.0894	.0203
Cd23C	CdS+ZnS+PbS	"	21	.1786		.0288
Cd21C	CdS+ZnS+PbS	"	21	.2593		.0367
Cd22C	CdS+ZnS+PbS	"	21	.3915		.0427
Cd27D	CdS+ZnS+PbS	660°C	70		.0215	.0017
Cd26D	CdS+ZnS+PbS	"	70		.0226	.0029
Cd25D	CdS+ZnS+PbS	"	70		.0427	.0083
Cd24D	CdS+ZnS+PbS	"	70		.0986	.0183
Cd23D	CdS+ZnS+PbS	"	70	.1930		.0196
Cd21D	CdS+ZnS+PbS	"	70	.2791		.0262
Cd22D	CdS+ZnS+PbS	"	70	.3233		.0303
Cd27E	CdS+ZnS+PbS	600°C	229		.0130	.0012
Cd26E	CdS+ZnS+PbS	"	229		.0200	.0029
Cd25E	CdS+ZnS+PbS	"	229		.0403	.0062
Cd24E	CdS+ZnS+PbS	"	229		.0993	.0117
Cd23E	CdS+ZnS+PbS	"	229	.1949		.0134
Cd21E	CdS+ZnS+PbS	"	229	.2702		.0198

Fig. 1. The condensed system CdS-PbS-ZnS at 740° C and vapor pressure of the system. (A) Representation of compositions of coexisting phases on ternary plot. All phase compositions fall on heavy side lines. Tie lines solid where determined experimentally, dashed were inferred. Three phase region stippled. (B) Plot of mole fraction CdS in galena vs mole fraction CdS in sphalerite or wurtzite. Open bars represent sphalerite-galena pairs; solid bars represent wurtzite-galena pairs. Dimensions of bars indicate analytical uncertainty. Metastable extensions of curves are dashed. Note four-fold expansion of galena scale. Open circle represents PbS-CdS binary point from Bethke and Barton (unpublished data).

1,020° C, is lowered with increasing CdS content (Kullerud, 1953), but the shape and position of the two phase field and the limit of CdS solubility in sphalerite are not known. The existence of CdS with the sphalerite structure (as the rare mineral hawleyite) suggests the possibility of extensive solid solution between the cubic modifications at low temperatures. The very slight solubility of PbS in the ZnS-CdS solid solutions, although it does not produce a detectable change in cell-edge, may have a significant effect on the shape and position of the PbS-saturated sphalerite-wurtzite two phase field, and so our ternary three phase data do not necessarily define the binary two phase region.

Procedures—Two series of runs were prepared to determine the mole fraction ratios $N_{CdS}^{sp}/N_{CdS}^{gn}$ and $N_{CdS}^{wz}/N_{CdS}^{gn}$ over a range of temperatures and bulk compositions. In the initial series the charges were prepared by adding varying amounts of CdS to a base mix containing 1:1 mole proportions of galena and sphalerite. After intimate mixing by grinding

in a power mortar each of the seven compositions prepared in this manner was split into five runs: 890°, 820°, 740°, 658°, and 600° C. Additional 890° C and 850° C isotherms were prepared in which approximately equal amounts of two wurtzite-greenockite solid solutions, whose compositions bracketed the expected final ZnS-CdS composition, were mixed with an appropriate amount of galena to produce a 1:1 mole ratio of galena to sphalerite or wurtzite. In this way the much slower reacting sphalerite or wurtzite approached its equilibrium composition from opposite directions. A close approach to equilibrium was assumed when single, sharp diffraction profiles were produced by the ZnS-CdS phase.

Results of Experiments.—The results and conditions of the various experiments are given in Table I and the experimental data are plotted in Figures 1 and 2. Mole fraction ratios for sphalerite-galena pairs are represented by open bars, and those for wurtzite-galena pairs by solid bars. The dimensions of the bars represent the uncertainty
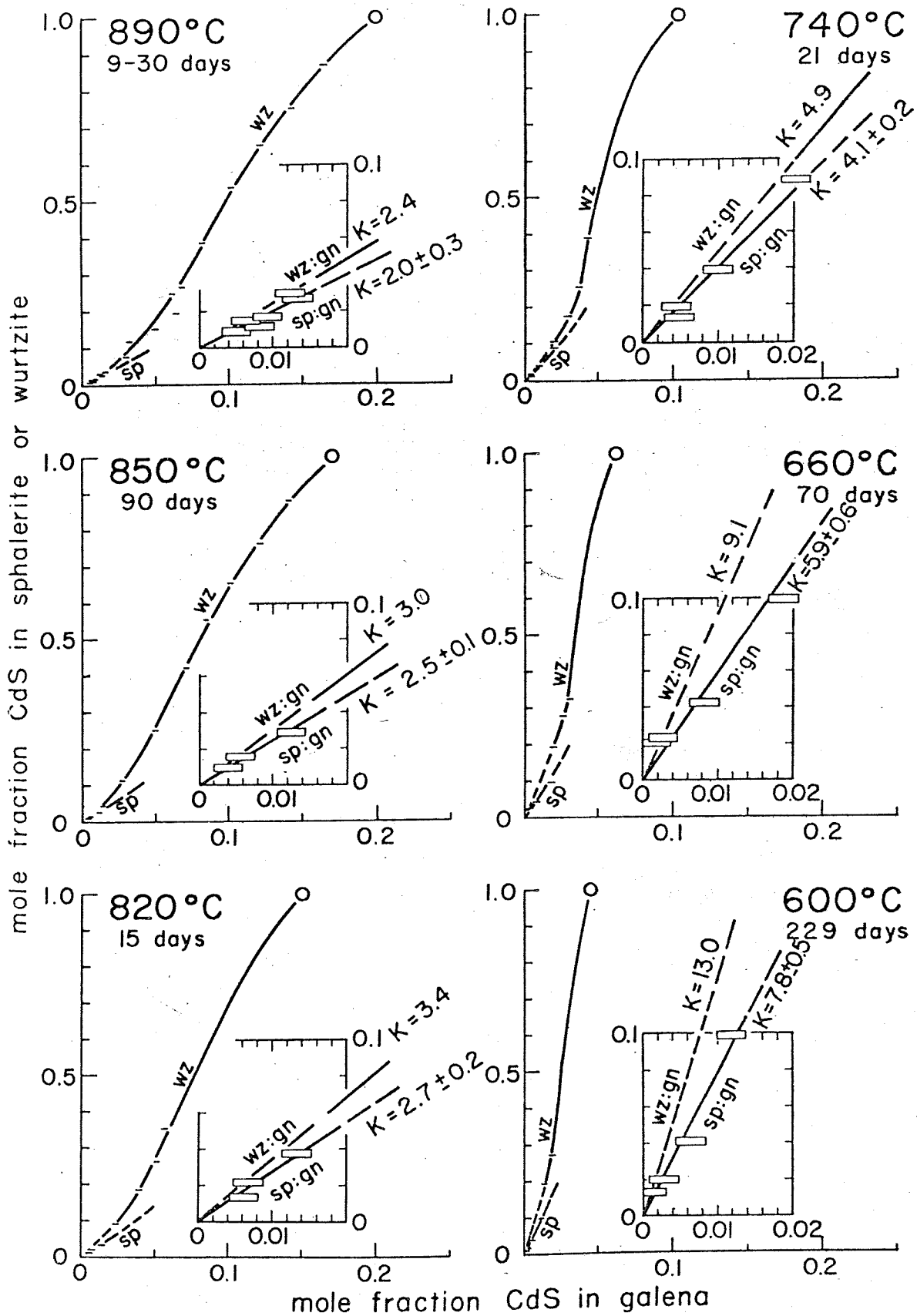
FIG. 2. Mole fraction CdS in galena vs mole fraction CdS in sphalerite or wurtzite. Experimental data at 6 temperatures. Construction and notation of main diagram as in Figure 1B. Inset diagrams show all sphalerite-galena runs.

of the analysis of composition. Note that the horizontal scale representing mole fraction CdS in galena is expanded 5 times over the vertical scale which represents the CdS content of sphalerite or wurtzite. In Figure 2 the region about the origin has been enlarged 5 times to better display the data points.

For each isotherm, the sphalerite-galena points were fit by linear regression to a straight line passing through the origin. The slope of this line is the mean value of the distribution coefficient. The uncertainty assigned to each distribution coefficient was estimated by assuming that lines representing the maximum and minimum values of the constant must pass through the origin and be within the band prescribed by one standard deviation from the mean throughout the range of our data. The data do not indicate any systematic variation from a straight line through the origin indicating that the mole fraction ratio is sensibly constant over the compositional range through which sphalerite is the stable ZnS phase. Thus both sphalerite and galena appear to exhibit Henry's law behavior at these temperatures.

The wurtzite-galena mole fraction ratios are seen, in each isotherm, to describe an S-shaped curve from the origin through the point representing the PbS-CdS binary solvus. The lower, dashed portions of these curves are metastable extensions into the sphalerite field, but must also pass through the origin. The curvature described by the wurtzite-galena data indicate that at moderate to high CdS contents the distribution coefficient is clearly a function of composition. We have drawn the metastable extensions of the curves to approximate straight lines through the origin in accordance with the expected approach to Henry's law behavior at low concentrations. Distribution coefficients for wurtzite-galena pairs were estimated by visual inspection with the assumption that the curve is approximately linear throughout most of the metastable range. Since no data were obtained in this range, such estimates are clearly less reliable than those for sphalerite-galena pairs. The uncertainty assigned to each wurtzite-galena distribution coefficient reflects our judgement as to the maximum and minimum slopes tolerated by the data.

The variation of the distribution coefficients $K_{CdS}^{sp\text{-}gn}$ and $K_{CdS}^{wz\text{-}gn}$ with temperature is illustrated in Figure 5A. A linear regression of unweighted values of log K on $1/T_{\circ K}$ was computed for each set of data. Although the sphalerite-galena data suggest curvature of the log K vs $1/T_{\circ K}$ relationship, we prefer the linear function illustrated, because in most reactions involving only solid phases

the enthalpy change of reaction may be assumed to be essentially constant over a rather broad range of temperature (Kubaschewski, Evans and Alcock, 1967, pp. 25–33). This assumption becomes increasingly tenuous upon extrapolation significantly beyond the experimental range. The 90% confidence interval was computed as part of the regression analysis on both data sets. That for the sphalerite-galena data is illustrated to indicate the uncertainty in the relationship between log K and $1/T_{\circ K}$. Because the wurtzite-galena relationship is geologically less significant, the 90% confidence interval has been omitted from the illustration. It is, however, narrower than that for the sphalerite-galena data, perhaps fortuitously so considering the method used to estimate the distribution coefficient at each temperature.

The slopes of the log K vs $1/T_{\circ K}$ relationships may be used to estimate the partial molar enthalpy change ($\Delta\bar{H}$) for the reactions:

$$CdS_{gn} \rightleftharpoons CdS_{sp} \tag{9}$$

and
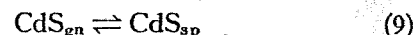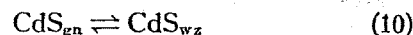
$$CdS_{gn} \rightleftharpoons CdS_{wz} \tag{10}$$

where CdS_{gn}, CdS_{sp} and CdS_{wz} represent CdS in galena, sphalerite and wurtzite structures at the temperature, pressure and composition range of our experiments. The values so estimated are listed in Table V. The uncertainties given were computed from the maximum and minimum slopes of straight lines lying wholly within the 90% confidence interval over the temperature range of the data.

Pressure corrections were calculated using molar volume data reported by Robie, Bethke and Beardsley (1967).[7] This calculation assumes that $\Delta\bar{V}$ and $\Delta\bar{H}$ do not change significantly over the P-T range of interest. This assumption appears reasonable since the log K vs $1/T$ plots may be considered essentially linear; the compressibilities of sulfides are quite low in general; and the coefficients of thermal expansion for cadmium-bearing sphalerites and galenas are very similar (Skinner, 1962). The pressure correction so calculated is very small, varying from $-6°$ C/kb at 200° C to $-11°$ C/kb at 600° C, and for most purposes can be neglected. The calculated correction has

---

[7] The value of a_0 for CdS of the rocksalt structure reported in Robie, Bethke and Beardsley (1967) was taken from Bethke and Barton (1961) and was based on a linear extrapolation of a_0 vs composition for CdS-bearing galenas. We have recently re-evaluated this relationship, and prefer an extrapolation based on a linear change in molar volume with composition. The corrected values, based on the linear molar volume extrapolation, for CdS of the rocksalt structure are: $a_0 = 5.488$A, $V_m = 24.89$ cm^3 or 0.5948 cal bar^{-1}. The corrected values were used in these calculations.

be assumed
broad range
and Alcock,
becomes in-
significantly
90% cor-
if the regres-
that for the
indicate the
n log K and
lationship is
confidence
stration. It
e sphalerite-
sidering the
n coefficient

relationships
lar enthalpy

(9)

(10)

resent CdS
tures at the
n range of
timated are
given were
mum slopes
n the 90%
ture range

using molar
ethke and
sumes that
y over the
on appears
ts may be
ressibilities
the coeffi-
m-bearing
(Skinner,
lculated is
at 200° C
t purposes
ection has

ure reported
from Bethke
xtrapolation
We have
r an extrap-
olume with
the linear
lt structure
bar⁻¹. The

een combined with the log K vs $1/T_{\circ K}$ relation-ship in Table V to define the *P-T* equation.

Although natural wurtzite is apparently always metastable, the data on the distribution of CdS between wurtzite and galena are geologically significant because they set a probable maximum limit to the potential error introduced by the occurrence of polytypes in natural sphalerites. The divergence of the two log K vs $1/T_{\circ K}$ relationships is sufficiently large to suggest that polytyping of natural sphalerites may introduce serious errors in the temperature estimate. The sense of such errors would be to indicate an apparent temperature lower than the actual temperature of deposition. In the absence of quantitative laboratory studies, a rough correction can perhaps be estimated if the relative proportions of sphalerite and wurtzite "layers" can be determined in the natural material, and the CdS content apportioned on this basis.

Discussion.—In Figure 11 we have plotted values of log K_{CdS}^{sp-gn} (converted to the more useful weight percent basis) against $1/T_{\circ K}$ and have made a linear extrapolation to 200° C. Neglecting, for the moment, the problems of such an extrapolation, the following points are evident: (1) even at temperatures as low as 200° C, galena formed in equilibrium with sphalerite containing a normal amount of CdS (1,000–3,000 ppm) would contain from 1–3 ppm CdS, an amount measurable by atomic absorption

techniques; and (2) the slope of the line permits a temperature estimate to a precision of approximately ±10–15° C at 300° C assuming an analytical uncertainty of ±10% of the amount present. If such a linear extrapolation, or a close approach thereto, is valid, the distribution of CdS between sphalerite and galena is potentially an attractive basis or precise geothermometry over a broad temperature range. The small correction for the effect of pressure enhances the attractiveness.

The linear extrapolation of the log K vs $1/T_{\circ K}$ relationship is probably reasonable to 100 C° or so below our experimental range, but beyond that it becomes increasingly tenuous. Our data serve to fix the *position* of the log K vs $1/T_{\circ K}$ curve rather well in the experimental range, but, at lower temperatures, the uncertainty in the *slope* becomes increasingly important, and the assumption that $\Delta \bar{H}$ remains essentially constant becomes increasingly less reliable.

In any event, it clearly remains necessary to determine the value of the distribution coefficient at low temperatures. Analytical difficulties due to the high values of the distribution constants together with sluggish reaction rates at temperatures below those investigated make an experimental approach to this problem very difficult. Empirical determination of distribution constants from natural materials utilizing independent tech-

TABLE II

EXPERIMENTAL DATA IN THE SYSTEM MnS-PbS-ZnS

A. Compositions of solid solutions used as starting materials in 850°C isotherm.

Batch	Mole fraction MnS	Mole fraction ZnS
Mn101	.0186	.9814
Mn102	.0405	.9595
Mn103	.0608	.9392
Mn105	.0997	.9003
Mn107	.2013	.7987
Mn108	.2995	.7005
Mn109	.3996	.6004
Mn110	.4984	.5016

B. Composition, temperature, duration, and results of runs.

| Run	Starting Materials	Temp. ±5°C	Time days	wz ±.002	sp ±.002	gn ±.002	Run	Starting Materials	Temp. ±5°C	Time days	wz ±.002	sp ±.002	gn ±.002
Mn101A	Mn102+ZnS+PbS	850°C	90		.0215	.0036	Mn27C	MnS+ZnS+PbS	740°C	21		.0231	.0020
Mn102A	Mn102+Mn101+PbS	"	90		.0306	.0038	Mn26C	MnS+ZnS+PbS	"	21		.0296	.0056
Mn103A	Mn103+Mn102+PbS	"	90	.0480	.0392	.0045	Mn25C	MnS+ZnS+PbS	"	21		.0704	.0060
Mn105A	Mn105+Mn103+PbS	"	90	.0746		.0074	Mn22C	MnS+ZnS+PbS	"	21	.1407		.0098
Mn107A	Mn107+ZnS+PbS	"	90	.0924		.0107	Mn24C	MnS+ZnS+PbS	"	21	.1474		.0098
Mn108A	Mn107+Mn105+PbS	"	90	.1400		.0160	Mn23C	MnS+ZnS+PbS	"	21	.2494		.0135
Mn109A	Mn108+Mn107+PbS	"	90	.2367		.0219	Mn21C	MnS+ZnS+PbS	"	21	.4011		.0188
Mn109A	Mn110+Mn109+PbS	"	90	.4377		.0292							
Mn110A	Mn110+PbS	"	90	.4870		.0353	Mn27D	MnS+ZnS+PbS	660°C	70		.0156	.0015
							Mn26D	MnS+ZnS+PbS	"	70		.0183	.0035
Mn B	MnS+ZnS+PbS	820°C	15		.0172	.0025	Mn25D	MnS+ZnS+PbS	"	70		.0510	.0032
Mn B	MnS+ZnS+PbS	"	15		.0355	.0049	Mn22D	MnS+ZnS+PbS	"	70	.1296		.0067
Mn B	MnS+ZnS+PbS	"	15		.0704	.0067	Mn24D	MnS+ZnS+PbS	"	70	.1536		.0079
Mn B	MnS+ZnS+PbS	"	15	.1585		.0177	Mn23D	MnS+ZnS+PbS	"	70	.2494		.0095
Mn B	MnS+ZnS+PbS	"	15	.2506		.0185							
Mn B	MnS+ZnS+PbS	"	15	.4226		.0260	Mn27E	MnS+ZnS+PbS	600°C	229		.0140	.0004
							Mn26E	MnS+ZnS+PbS	"	229		.0263	.0014
							Mn22E	MnS+ZnS+PbS	"	229		.1038	.0055
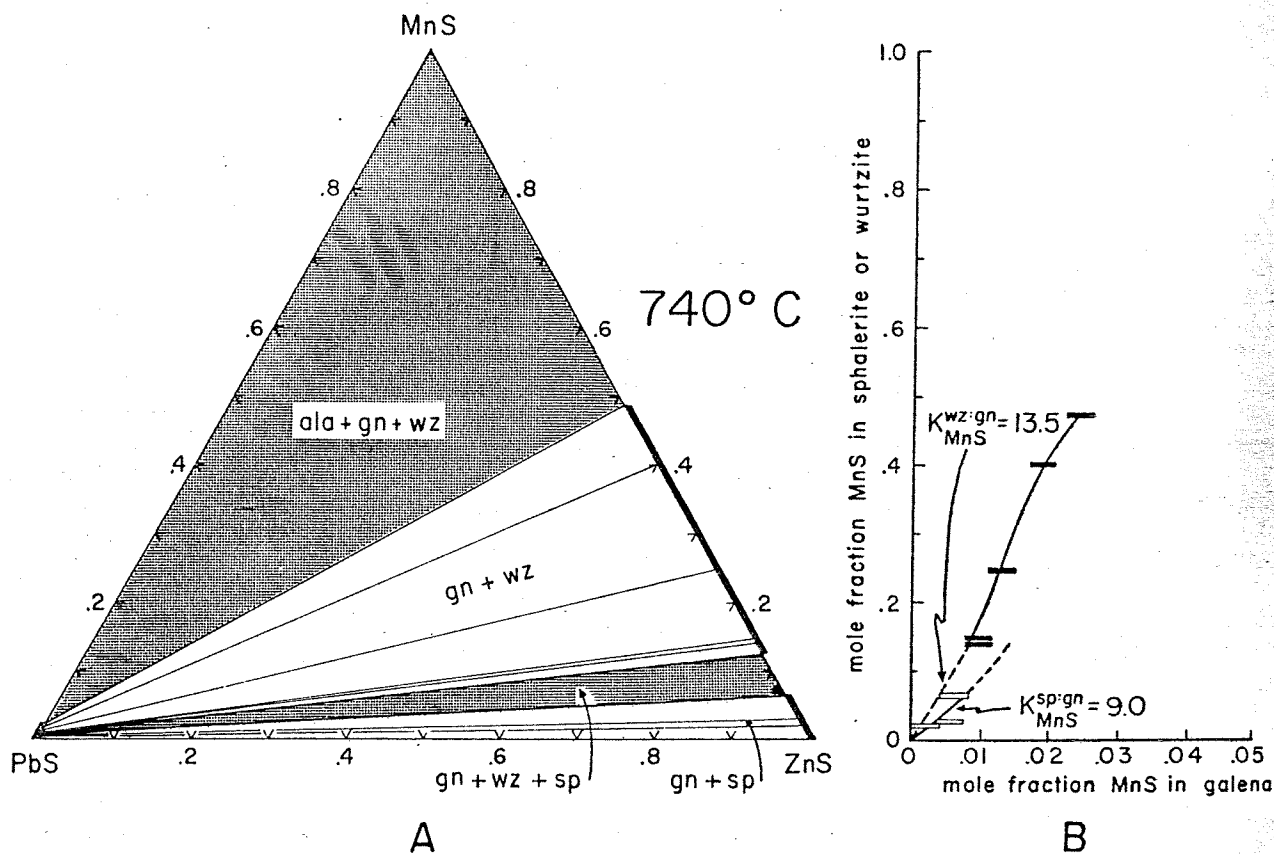
FIG. 3. The condensed system MnS-PbS-ZnS at 740° C and vapor pressure of the system. (A) Representation of composi-
tions of coexisting phases on ternary plot. All phase compositions fall on heavy side lines. Tie lines determined experimentally.
Three phase regions stippled. (B) Plot of mole fraction MnS in galena vs mole fraction MnS in sphalerite or wurtzite. Open
bars represent sphalerite-galena pairs; solid bars represent wurtzite-galena pairs. Dimensions of bars indicate analytical un-
certainty. Metastable extension of wurtzite-galena pairs dashed. Note ten-fold expansion of galena scale.

niques of geothermometry is perhaps the most
promising approach. Comparison with filling
temperatures of fluid inclusions appears particu-
larly promising, and we are currently pursuing
such studies on material from Creede, Colorado.

Distribution of Manganese between Sphalerite or Wurtzite and Galena

The distribution of MnS between sphalerite
or wurtzite and galena may be described in terms
of the system MnS-PbS-ZnS (Fig. 3A). The
system is analogous to the system CdS-PbS-ZnS
just described, and was handled in essentially the
same manner. At the temperatures of our experi-
ments, the system contains 4 solid phases: an MnS-
bearing galena solid solution, an MnS-bearing
sphalerite solid solution, an MnS-bearing wurtzite
solid solution, and essentially pure alabandite.
As in the previous system, the solubility of galena
in the ZnS-MnS solid solutions is too small to affect
our analyses as is the solubility of ZnS in galena.

The solubility of MnS in galena is considerably
smaller than that of CdS. Incomplete experiments
indicate that the maximum solubility is about
3.5 mole percent. Several investigators have
studied the ZnS-MnS binary (Kroger, 1938; 1939;
Kullerud, 1953; Juza et al., 1956; B. J. Skinner,
personal communication, 1962). The system differs
from the ZnS-CdS binary in that, in the range of
our experiments, a miscibility gap appears at about
50 mole percent between manganese-bearing wurtz-
ite and alabandite. The wurtzite solvus is quite
steep, decreasing about 85° C per mole percent
MnS. The sphalerite-wurtzite two-phase field
also plunges steeply, the limit of sphalerite stability
being approximately 7 mole percent MnS at 600° C.
As in the previous system, the slight solubility
of PbS in the ZnS-MnS solid solutions may have a
significant affect on this two-phase field, and there-
fore our data cannot necessarily be compared
directly with the binary.

Procedures.—Two series of runs were prepared
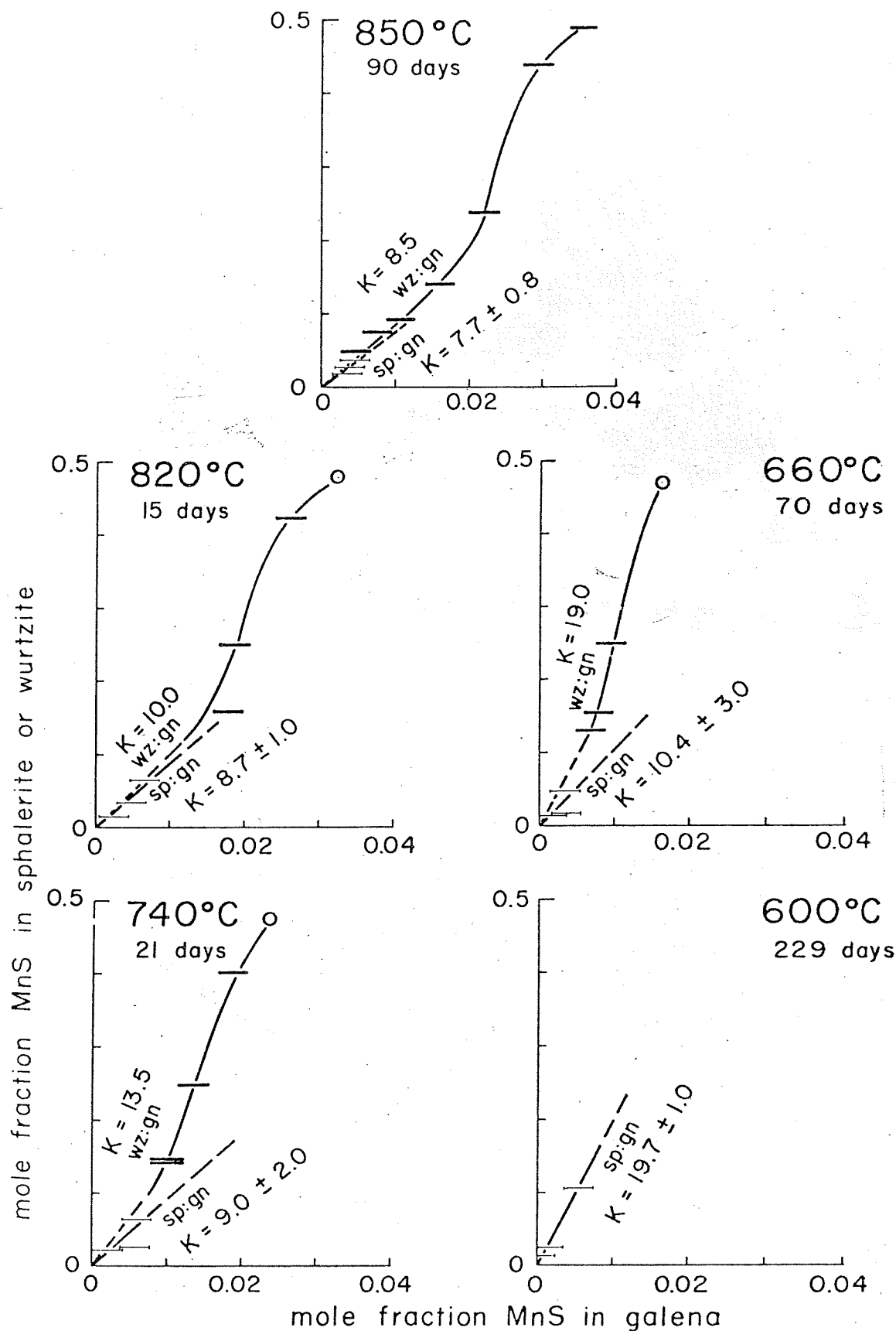to determine the mole fraction ratios $N_{MnS}^{sp}/N_{MnS}^{gn}$

FIG. 4. Mole fraction MnS in galena vs mole fraction MnS in sphalerite or wurtzite. Experimental data at 5 temperatures. Construction and notation as in Figure 3B. Three phase (ala + wz + gn) points taken from PbS − MnS binary (Bethke and Barton, unpublished) are shown as open circles.
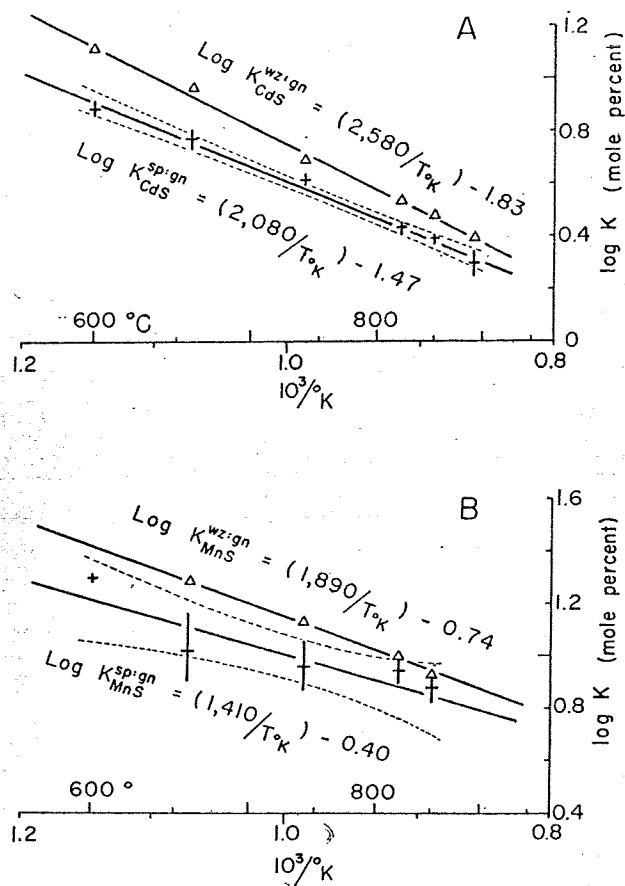
149

$$\log K_{CdS}^{wz \cdot gn} = (2{,}580/T_{^\circ K}) - 1.83$$

$$\log K_{CdS}^{sp \cdot gn} = (2{,}080/T_{^\circ K}) - 1.47$$

$$\log K_{MnS}^{wz \cdot gn} = (1{,}890/T_{^\circ K}) - 0.74$$

$$\log K_{MnS}^{sp \cdot gn} = (1{,}410/T_{^\circ K}) - 0.40$$

Fig. 5. Variation of distribution coefficients with temperature. (A) Distribution of CdS between sphalerite and galena and wurtzite and galena. (B) Distribution of MnS between sphalerite and galena and wurtzite and galena. Size of crosses indicates uncertainty in estimation of distribution coefficients and $\pm 5^\circ$ C uncertainty in temperature for sphalerite-galena data. Uncertainties in wurtzite-galena data not shown. 90 percent confidence interval indicated by dashed lines.

and $N_{MnS}^{wz}/N_{MnS}^{gn}$ over a range of temperatures and bulk compositions. In the initial series the charges were compounded by adding various amounts of alabandite to a 1:1 base mix of galena and sphalerite, and intimately mixing each batch in a power mortar. Each batch was then split into 5 isotherms: 890°, 820°, 740°, 658° and 600° C. The 890° C runs showed evidence of melting and were discarded. Consequently an 850° C isotherm was prepared from pure galena and a mixture of two MnS-bearing wurtzite solid solutions which bracketed the expected final composition of the ZnS-MnS phase.

Results of Experiments.—Our experimental data for the distribution of MnS between sphalerite or wurtzite and galena are presented in Table II and illustrated in Figures 3 and 4. In these figures the coordinate representing the MnS content of galena is expanded 10 times over that representing

the MnS content of sphalerite or wurtzite. Our interpretation of the MnS data is essentially the same as for the analogous CdS data. We assume that all sphalerite-galena pairs exhibit Henry's law behavior at the temperatures of our experiments because the data points (represented by narrow bars in Fig. 3 and 4) are compatible with straight lines through the origin. The distribution coefficient and its associated uncertainty were estimated for each isotherm in a manner identical to the procedure used in the previous system. The degree of fit of the sphalerite-galena data is clearly not as good as in the previous system due, in part, to the greater magnitude of the distribution coefficient, but also probably because of a less close approach to equilibrium due to the relative inertness of MnS in dry systems.

The wurtzite-galena points are seen to lie along S-shaped curves from the lower limit of wurtzite stability through the points representing the alabandite-galena-wurtzite field. The degree of fit of the wurtzite-galena data points to this curve is approximately the same as in the previous system. Again, the curve was constructed to approach a straight line through the origin in the dashed, metastable region, consistent with a close approach to Henry's law behavior in that range. The distribution coefficients K_{MnS}^{sp-gn} and K_{MnS}^{wz-gn} and the uncertainties assigned to them again were estimated in an identical manner to those describing the distribution of CdS between these phases.

The relationship between the distribution coefficients and temperature is illustrated in Figure 5B. A linear regression of $\log K$ on $1/T_{^\circ K}$ was computed for each set of data using the same assumptions as in the previous system, and the resulting expressions are given on Figure 5B. The scatter of $\log K$ values about the straight line is considerably larger than for the previous system, and the 90% confidence interval much broader. The $\log K_{MnS}^{wz-gn}$ points on the other hand, exhibit about the same degree of scatter as do the $\log K_{CdS}^{wz-gn}$ and the 90% confidence interval (again not illustrated) on the wurtzite-galena relationship is much narrower than on the sphalerite-galena line. Again, the wurtzite-galena data serve to indicate the possible error introduced by polytyping in natural sphalerites. The change in partial molar enthalpies calculated for the two distribution reactions are listed in Table V.

Pressure corrections calculated from the molar volume data of Robie, Bethke and Beardsley (1967)[3] ranged from -9°/kb at 200° C to -16°/kb

[8] The value for the partial molar volume of MnS in sphalerite used in these calculations was computed by extrapolating the corrected relationship between a_0 and MnS content of sphalerite (footnote 5) to pure MnS. The values so
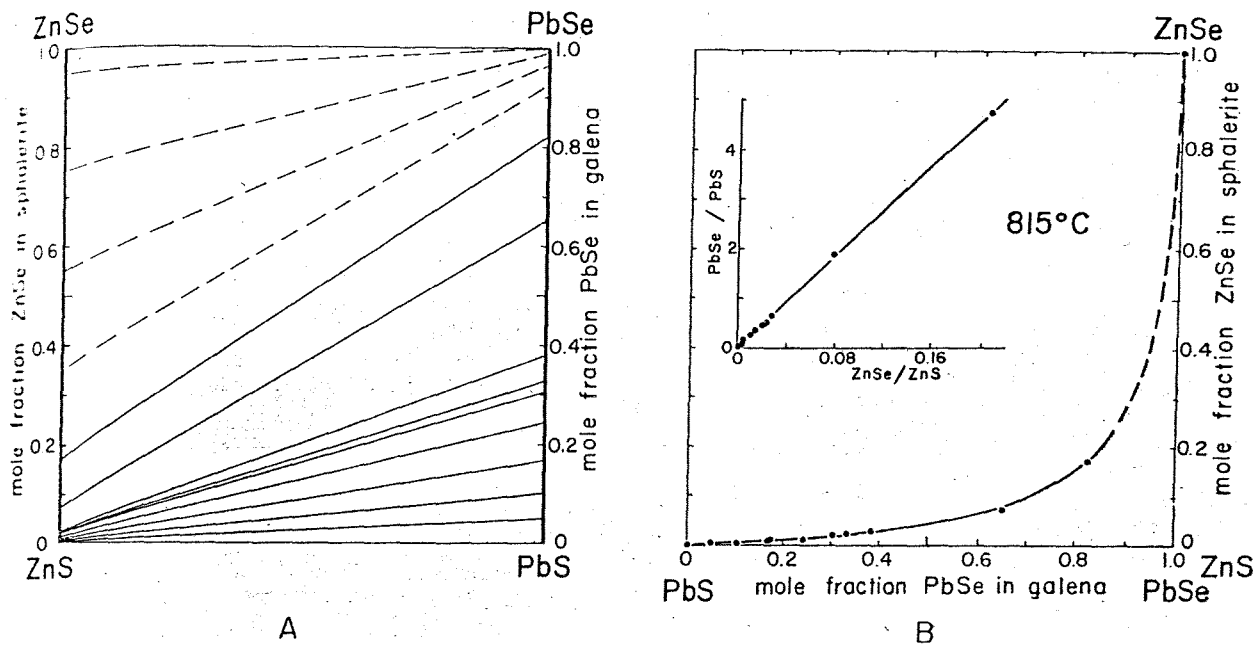
FIG. 6. The condensed system PbS-PbSe-ZnS-ZnSe at 815° C and vapor pressure of the system. (A) Representation of compositions of coexisting sphalerite and galena solid solutions on quaternary plot. All phase compositions fall along heavy side lines. Tie lines solid where determined experimentally, dashed where inferred. (B) Mole fraction ZnSe in sphalerite vs mole fraction PbSe in galena. Size of circles approximately 2 times analytical uncertainty. Inset is plot of same data computed as mole fraction ratios PbSe/PbS and ZnSe/ZnS allowing direct estimation of distribution coefficient from slope of line through origin and points.

at 600° C. This correction is still small, and in many instances can be neglected. The combined P-T expressions for the distribution of MnS between sphalerite and galena and wurtzite and galena are given in Table V.

Discussion.—Values of log $K_{\text{MnS}}^{\text{sp-gn}}$ converted to a weight percent basis are plotted in Figure 11, and extended to 200° C assuming a linear extrapolation. Considering the large width of the 90% confidence interval in Figure 5B together with the assumption of constant $\Delta \bar{H}$, such an extrapolation is semi-quantitative at best, and, even more than in the previous system, data at low temperatures are required. The extrapolation is presented only to indicate that it falls within the same range as that for $K_{\text{CdS}}^{\text{sp-gn}}$ and therefore the distribution of MnS between sphalerite and galena is potentially useful and worthy of further calibration.

Distribution of Selenium between Galena and Sphalerite

We may refer our discussion of the distribution of selenium between sphalerite and galena to the system PbS-PbSe-ZnS-ZnSe (Fig. 6). Both sphal-

determined are $a_0 = 5.596$A, $V_m = 26.385$ cm³ or 0.60359 cal bar⁻¹. These values differ from those reported in Robie, Bethke and Beardsley (1967) which were taken from Skinner's incorrect relationship.

erite-stilleite and galena-clausthalite form complete binary solid solutions at the temperatures of our experiments. The mutual solubility of PbSe and ZnSe and of PbS and ZnS is too small to bias our compositional analyses. Both solid solution series are, for purposes of this study, stoichiometric with respect to metal:anion ratio. Thus the compositions of all crystalline phases in the system lie on the two heavy side lines in Figure 6A. The system constitutes a reciprocal salt pair and thus is ternary although represented in Figure 6 in terms of four components. The reaction describing the distribution is the exchange reaction:

$$PbS + ZnSe \rightleftharpoons PbSe + ZnS \qquad (11)$$
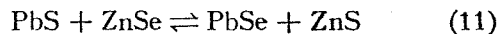
and the distribution coefficient has the form:

$$K_{\text{Se}}^{\text{gn-sp}} = \frac{N_{\text{PbSe}}^{\text{gn}} \cdot N_{\text{ZnS}}^{\text{sp}}}{N_{\text{PbS}}^{\text{gn}} \cdot N_{\text{ZnSe}}^{\text{sp}}} = K_{\text{reaction}} \cdot \frac{\gamma_{\text{PbSe}}^{\text{gn}} \cdot \gamma_{\text{ZnSe}}^{\text{sp}}}{\gamma_{\text{PbSe}}^{\text{gn}} \cdot \gamma_{\text{ZnS}}^{\text{sp}}} \qquad (12)$$

where K_{reaction} is the standard equilibrium constant for reaction (11).

Procedures.—Runs in this system were prepared in two ways. The 815° and 700° C isotherms were compounded using opposing end members, either PbS + ZnSe or PbSe + ZnS, as starting materials. The 890°, 740°, 658° and 600° C isotherms were prepared from mixtures of pure PbS and ZnS-ZnSe solid solutions of various compositions. The condi-

TABLE III

EXPERIMENTAL DATA IN THE SYSTEM PbS-PbSe-ZnS-ZnSe

A. Composition of ZnS-ZnSe solid solutions used as starting
materials in 890°C, 740°C, 660°C, and 600°C isotherms.

Batch	Mole fraction ZnSe	Mole fraction ZnS
Se105	.0772	.9228
Se106	.3004	.6996
Se107	.4984	.5016
Se108	.7711	.2289
Se109	.6922	.3078
Se110	.4093	.5903
Se111	.3335	.6665
Se112	.1430	.8570

B. Composition, temperature, duration, and results of runs.

Run	Starting Materials	Temp. ±5°C	Time days	Mole fraction PbSe in gn ±.002	Mole fraction ZnSe in sp ±.002	Run	Starting Materials	Temp. ±5°C	Time days	Mole fraction PbSe in gn ±.002	Mole fraction ZnSe in sp ±.002
Se1A	Se105+PbS	890°C	13	.077	.006	Se6C	Se110+PbS	740°C	21	.392	.019
Se8A	Se112+PbS	"	13	.160	.011	Se3C	Se107+PbS	"	21	.490	.028
Se7A	Se111+PbS	"	13	.321	.029	Se5C	Se109+PbS	"	21	.582	.034
Se2A	Se106+PbS	"	13	.325	.027	Se4C	Se108+PbS	"	21	.729	.056
Se6A	Se110+PbS	"	13	.397	.037						
Se3A	Se107+PbS	"	13	.453	.053	Se82	PbSe+ZnS	700°C	70	.341	.009
Se5A	Se109+PbS	"	13	.551	.070	Se83	PbSe+ZnS	"	70	.679	.040
Se4A	Se108+PbS	"	13	.682	.123	Se85	PbS+ZnSe	"	70	.878	.122
						Se84	PbSe+ZnS	"	70	.883	.124
Se71	PbSe+ZnS	815°C	27	.050	.004						
Se51	PbSe+ZnS	"	19	.102	.004	Se7D	Se111+PbS	660°C	70	.336	.011
Se55	PbSe+ZnS	"	19	.168	.011	Se2D	Se106+PbS	"	70	.340	.013
Se72	PbSe+ZnS	"	27	.172	.011	Se6D	Se110+PbS	"	70	.392	.019
Se52	PbSe+ZnS	"	19	.242	.015	Se3D	Se107+PbS	"	70	.488	.013
Se56	PbSe+ZnS	"	19	.305	.019	Se5D	Se109+PbS	"	70	.595	.024
Se73	PbSe+ZnS	"	27	.333	.022	Se4D	Se108+PbS	"	70	.749	.040
Se53	PbSe+ZnS	"	19	.382	.026						
Se74	PbSe+ZnS	"	27	.651	.072	Se2E	Se106+PbS	600°C	210	.308	.004
Se75	PbSe+ZnS	"	27	.825	.170	Se6E	Se110+PbS	"	210	.403	.006
						Se3E	Se107+PbS	"	210	.501	.010
Se8C	Se112+PbS	740°C	21	.136	.005	Se5E	Se109+PbS	"	210	.600	.014
Se7C	Se111+PbS	"	21	.336	.014	Se4E	Se108+PbS	"	210	.752	.027
Se2C	Se106+PbS	"	21	.346	.016						

tions of the experiments, starting materials and compositions of the reaction products are listed in Table III.

Results of Experiments.—The results of our experiments on the distribution of selenium between sphalerite and galena are illustrated in Figures 6 and 7. In Figure 6A tie lines determined at 815° C are plotted. In Figure 6B, the mole fraction PbSe in galena is plotted against mole fraction ZnSe in sphalerite in the major portion of the diagram. The points fall on a smooth, symmetrical curve for which the ratio:

$$\frac{N^{gn}_{PbSe} \cdot N^{sp}_{ZnS}}{N^{gn}_{PbS} \cdot N^{sp}_{ZnSe}} = K^{gn-sp}_{Se} \qquad (13)$$

is constant over the compositional range investigated. This constancy of the mole fraction ratio is better illustrated in the insert in Figure 6B where $N^{gn}_{PbSe}/N^{gn}_{PbS}$ is plotted directly against $N^{sp}_{ZnSe}/N^{sp}_{ZnS}$. In Figure 7 plots similar to this inset are presented for each isotherm showing that the mole fraction ratio is independent of composition at least down to 600° C. Straight lines through the origin were fit to the data by the method of least squares, and the slope of this line is the numerical value of K^{gn-sp}_{Se}. The reported uncertainty was calculated in the same manner as described for the cadmium distribution coefficients.

The fact that the mole fraction ratio is constant at each temperature, over the entire compositional range investigated, means that the activity coefficient ratio must also be constant. This suggests that both solid solutions behave ideally over the composition and temperature range investigated.

Alternatively, fortuitous, mutually compensating deviation from ideality in both phases could give rise to the apparently ideal behavior. Since the behavior is maintained over a temperature range of nearly 300° C, we strongly prefer the first alternative.

At low concentrations the values of N_{PbS}^{gn} and N_{ZnS}^{sp} are nearly unity and therefore have little effect on the numerical value of the distribution coefficient. Therefore, for assemblages containing only small amounts of selenium, the reduced distribution coefficient

$$K_{Se}^{'gn-sp} = \frac{PbSe_{gn}}{ZnSe_{sp}} \qquad (14)$$

will yield numerical values well within the precision of analysis, and is much more convenient.

Wurtzite was not produced in any of our runs and therefore we cannot predict the effect of polytyping of natural sphalerite on temperature estimates based on the distribution of selenium between sphalerite and galena.

In Figure 10A the logarithm of the distribution constant is plotted against the reciprocal of the absolute temperature. The straight line through the points computed as in the previous systems describes the temperature dependence of the distribution constant, and its analytical expression is noted on the figure. The 90% confidence interval is also illustrated. If both solid solutions are assumed to behave ideally, the ΔH of the distribution reaction calculated from the slope of the log K vs $1/T_{°K}$ plot is $-13,030 \pm 1,500$ calories per mole, which is not inconsistent with the 25° C value of $-9,700 \pm 4,200$ calories calculated from the heats of formation of the phases given by Kubaschewski, Evans, and Alcock (1967).

A pressure correction of slightly more than $+1°/1,000$ bars at 600° C was calculated from the molar volume data (Robie, Bethke and Beardsley, 1967), and can obviously be neglected for any practical application.

Discussion.—Values of log K converted to a weight percent basis are plotted against $1/T_{°K}$ in Figure 11. The straight line describing the data has a greater slope than those for either the cadmium or manganese bearing systems. Assuming the validity of such a linear extrapolation, the slope should allow temperature estimates to a precision of $\pm 10°$–$15°$ C for those assemblages to which it can be applied. At lower temperatures the values of the distribution coefficient are quite high, reaching 1,000:1 at approximately 375° C. Although the selenium content of some ores may reach several percent, the element is most commonly present in only trace amounts. We may
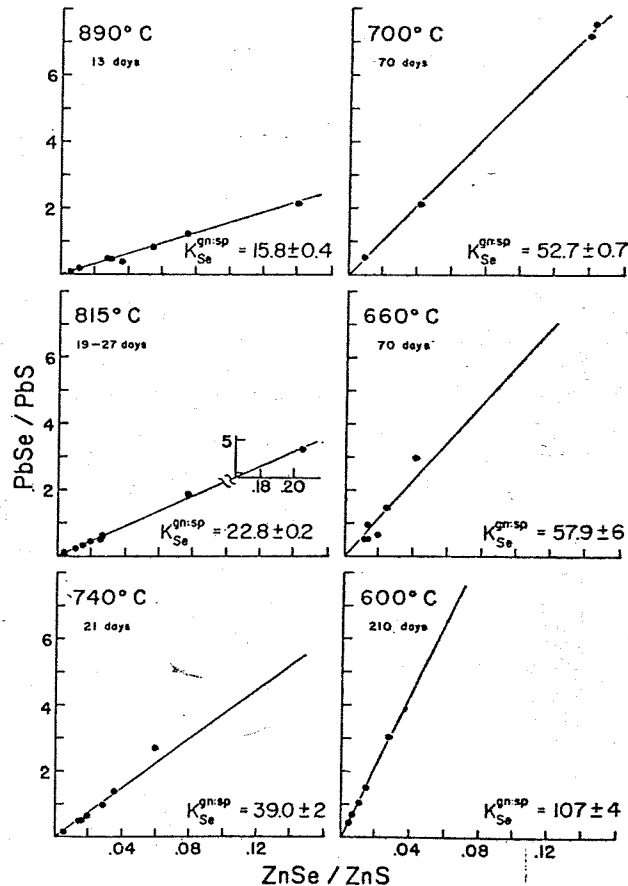

FIG. 7. Plots of mole fraction ratios PbSe/PbS vs ZnSe/ZnS calculated from experimental data for 6 temperatures. Construction and notation as for inset in Figure 6B.

therefore expect that the distribution of selenium between sphalerite and galena will not be as universally applicable as that of manganese and, in particular, cadmium.

The validity of the linear extrapolation of the selenium distribution data to lower temperatures is just as questionable as in the previous systems. A recent attempt by Halbig (1969) to measure the distribution coefficient at temperatures down to 300° C has yielded results at considerable variance with ours. Halbig's data were gathered by recrystallizing PbS and ZnS in a 2 molar NaOH aqueous solution doped with Se[75] radioisotope added as $HSeO_3$, followed by separation of the phases and radiometric analysis. His data also yield a linear relationship between log K and $1/T_{°K}$, but the slope of this line is much lower than ours, and in the range of overlap Halbig's data indicate a distribution coefficient significantly lower than ours. Mutual discussions have failed as yet to resolve the reasons for the differences in our results, but we see no reason for abandoning our values.

Distribution of Selenium between Galena and Chalcopyrite

Preliminary experiments were conducted on the distribution of selenium between galena and chalcopyrite. In gross aspects the system is analogous to the distribution of selenium between galena and sphalerite. However, at higher selenium contents the chalcopyrite-eskebornite (in the sense of Tischendorf, 1960) join becomes nonbinary, thus limiting the extent of solid solution. In the runs prepared for spacing curve standards, compositions greater than 36.7 mole percent eskebornite yielded spurious phases at 600° C. No further attempt was made to clarify the relations along this join as it was felt the complexities of the system Cu-Fe-S were sufficient without introducing selenium as an additional component. An additional complication is the departure of chalcopyrite from the ideal $CuFeS_2$ composition at high temperatures, both with respect to the Cu:Fe and metal:anion ratio. For this study we chose to use chalcopyrite of a 1:1 Cu to Fe ratio and a 1.052:1 metal to anion ratio. Chalcopyrite of these proportions is stable over the temperature and compositional ranges investigated. The reaction describing the distribution is most conveniently written to include one mole of selenium on each side of the equation:

$$PbS + Cu_{0.526}Fe_{0.526}Se \rightleftharpoons$$

$$PbSe + Cu_{0.526}Fe_{0.526}S \quad (15)$$
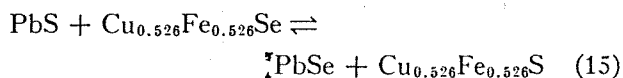
TABLE IV

EXPERIMENTAL DATA IN THE SYSTEM PbS-PbSe-Cu$_{.526}$Fe$_{.526}$S-Cu$_{.526}$Fe$_{.526}$Se

A. Composition of runs.

Run	Composition
Ccp95B,C,D,F	Cu$_{.526}$Fe$_{.526}$S$_{.947}$Se$_{.053}$ + PbS
Ccp96B,C,D,F	Cu$_{.526}$Fe$_{.526}$S$_{.895}$Se$_{.105}$ + PbS
Ccp97B,C,D,F	Cu$_{.526}$Fe$_{.526}$S$_{.747}$Se$_{.253}$ + PbS
Ccp98B,C,D,F	Cu$_{.526}$Fe$_{.526}$S$_{.632}$Se$_{.368}$ + PbS

B. Temperature, duration, and results of runs.

Run no.	Temp. ±5°C	Time days	PbSe in galena ±.002	Mole fraction Cu$_{.526}$Fe$_{.526}$Se in chalcopyrite ±.003
Ccp95B	595°C	10	.089	.011
Ccp96B	"	10	.167	.015
Ccp97B	"	10	.423	.033
Ccp98B	"	10	.643	.050
Ccp95C	550°C	12	.091	.008
Ccp96C	"	12	.171	.008
Ccp97C	"	12	.435	.018
Ccp98C	"	12	.597	.030
Ccp95D	475°C	30	.090	.000
Ccp96D	"	30	.200	.005
Ccp97D	"	30	.473	.011
Ccp98D	"	30	.639	.013
Ccp95F	390°C	72	.090	.000
Ccp96F	"	72	.313	.000
Ccp97F	"	72	.533	.003
Ccp98F	"	72	.654	.005

The distribution coefficient is thus:

$$K_{Se}^{gn:ccp} = \frac{N_{PbSe}^{gn} \cdot N_{Cu_{0.526}Fe_{0.526}S}^{ccp}}{N_{PbS}^{gn} \cdot N_{Cu_{0.526}Fe_{0.526}Se}^{ccp}}$$

$$= K_{reaction} \cdot \frac{\gamma_{PbS}^{gn} \cdot \gamma_{Cu_{0.526}Fe_{0.526}Se}^{ccp}}{\gamma_{PbSe}^{gn} \cdot \gamma_{Cu_{0.526}Fe_{0.526}S}^{ccp}} \quad (16)$$

Procedures.—Tie lines relating the composition of galena-clausthalite solid solutions to those on the chalcopyrite-eskebornite join were determined for four compositions at each of four temperatures: 595°, 550°, 475° and 390° C. The runs were compounded from pure PbS and various chalcopyrite-eskebornite solid solutions, ground together in batches and split into the four isotherms. The starting compositions and conditions of each run and the composition of the reaction products are listed in Table IV. The short duration of the runs (10 to 72 days) and the comparatively low temperature range are particularly notable.

Results of Experiments.—The results of our experiments listed in Table IV and illustrated in Figures 8 and 9 clearly show that selenium is concentrated in galena relative to chalcopyrite. However, in contrast to the previously described distribution of selenium between galena and sphalerite wherein the distribution coefficient is independent of composition, Figure 8 shows that the true distribution coefficient

$$(K = N_{PbSe}^{gn} \cdot N_{Cu_{0.526}Fe_{0.526}S}^{ccp} / N_{PbS}^{gn} \cdot N_{Cu_{0.526}Fe_{0.526}Se}^{ccp})$$

clearly increases with increasing selenium content. Surprisingly, the reduced distribution coefficient $(K' = N_{PbSe}^{gn} / N_{Cu_{0.526}Fe_{0.526}Se}^{ccp})$ gives a better fit to the data and is independent of selenium content at the concentration levels investigated. We shall use the reduced distribution coefficient to describe the distribution of selenium between galena and chalcopyrite, but for reasons discussed below we shall limit its application to the compositional range of our experiments.

Discussion.—The slope and position of the straight line describing the temperature dependence of the reduced distribution coefficients as plotted in Figure 11 would appear to provide an excellent basis for geothermometry, but three important factors place severe limitations on the potential usefulness of this relationship.

To explain the first difficulty let us further consider the typical isotherm shown in Figure 8. We have noted that the true distribution coefficient, K, is not independent of composition in contrast to the data on the distribution of selenium between galena and sphalerite, whereas the reduced distribution coefficient, K', is apparently constant over the

TABLE V

SUMMARY OF DISTRIBUTION COEFFICIENTS AS FUNCTIONS OF TEMPERATURE AND PRESSURE

$$\log K = \frac{-\Delta \bar{H} - \Delta \bar{V} P}{2.3RT} + C$$

	Reaction	Distribution coefficient	Mole fraction	Weight percent	1/ $\Delta \bar{H}$ cal mole⁻¹	2/ $\Delta \bar{V}$ cal bar⁻¹	Temperature range of experiments
(1)	$CdS_{gn} \rightleftharpoons CdS_{sp}$	$K^{sp-gn}_{CdS} = \frac{CdS_{sp}}{CdS_{gn}}$	$\log K = \frac{2080-.0264P}{T°K} -1.47$	$\log K = \frac{2080-.0264P}{T°K} -1.08$	-9,500±1,050	0.1194±.0008	600-890°C
(2)	$CdS_{gn} \rightleftharpoons CdS_{wz}$	$K^{wz-gn}_{CdS} = \frac{CdS_{wz}}{CdS_{gn}}$	$\log K = \frac{2580-.0268P}{T°K} -1.83$	$\log K = \frac{2580-.0268P}{T°K} -1.54$	-12,220±1,500	0.1207±.0006	600-890°C
(3)	$MnS_{gn} \rightleftharpoons MnS_{sp}$	$K^{sp-gn}_{MnS} = \frac{MnS_{sp}}{MnS_{gn}}$	$\log K = \frac{1410-.0261P}{T°K} -0.40$	$\log K = \frac{1410-.0261P}{T°K} -0.01$	-6,440±4,110	0.1177±.0005	600-850°C
(4)	$MnS_{gn} \rightleftharpoons MnS_{wz}$	$K^{wz-gn}_{MnS} = \frac{MnS_{wz}}{MnS_{gn}}$	$\log K = \frac{1890-.0278P}{T°K} -0.74$	$\log K = \frac{1890-.0278P}{T°K} -0.35$	-10,300±5,000	0.1274±.0003	660-850°C
(5)	$PbS_{gn}+ZnSe_{sp} \rightleftharpoons PbSe_{gn}+ZnS_{sp}$	$K^{gn-sp}_{Se} = \frac{PbSe_{gn}·ZnS_{sp}}{PbS_{gn}·ZnSe_{sp}}$	$\log K = \frac{2850+.0027P}{T°K} -1.24$	$\log K = \frac{2850+.0027P}{T°K} -1.33$	-13,030±1,500	0.0125±.0003	600-890°C
(6)	$PbS_{gn}+Cu_{0.526}Fe_{0.526}Se_{ccp} \rightleftharpoons PbSe_{gn}+Cu_{0.526}Fe_{0.526}S_{ccp}$	3/ $K^{gn-ccp}_{Se} = \frac{PbSe_{gn}}{Cu_{0.526}Fe_{0.526}Se_{ccp}}$	$\log K = \frac{3410}{T°K} -2.85$	$\log K = \frac{3410}{T°K} -3.10$	-15,580±1,050	——	300-595°C
(7)	$Cu_{0.526}Fe_{0.526}S_{ccp}+ZnSe_{sp} \rightleftharpoons Cu_{0.526}Fe_{0.526}Se_{ccp}+ZnS_{sp}$	3/ $K^{ccp-sp}_{Se} = \frac{Cu_{0.526}Fe_{0.526}Se_{ccp}}{ZnSe_{sp}}$	$\log K = \frac{-560}{T°K} +1.61$	$\log K = \frac{-560}{T°K} +1.77$	+2,650±1,300	——	Calculated from (5) and (6)

1/ Calculated from experimental data by relation (6) in text.
2/ Calculated from data in Robie, Bethke, and Beardsley (1967).
3/ Emperical constants, see text.

$$K' = \frac{PbSe}{Cu_{.526}Fe_{.526}Se} = 12$$

$$K = \frac{PbSe \cdot Cu_{.526}Fe_{.526}S}{PbS \cdot Cu_{.526}Fe_{.526}Se} = 12$$

A

$$K = \frac{PbSe \cdot Cu_{.526}Fe_{.526}S}{PbS \cdot Cu_{.526}Fe_{.526}Se} = 12$$

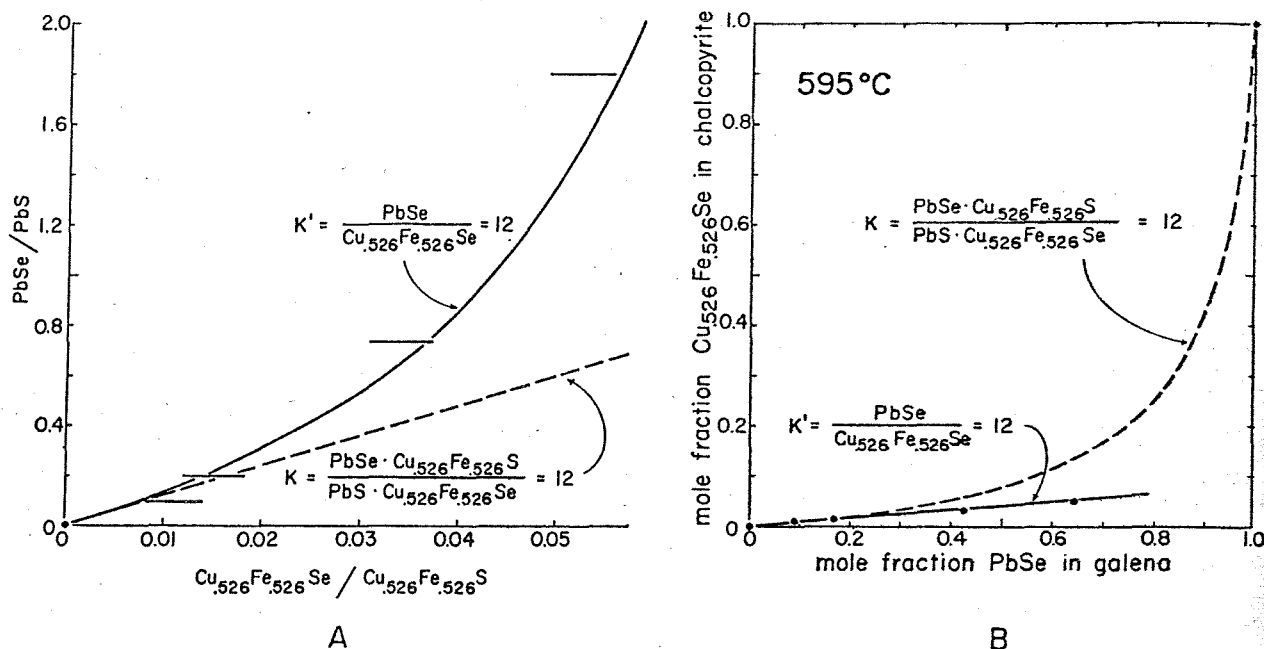$$K' = \frac{PbSe}{Cu_{.526}Fe_{.526}Se} = 12$$

595 °C

B

FIG. 8. The distribution of selenium between galena and chalcopyrite at 595° C. (A) Plot of mole fraction ratios $PbSe/PbS$ vs $Cu_{0.526}Fe_{0.526}Se/Cu_{0.526}Fe_{0.526}S$. Dimensions of bars indicate analytical uncertainty. (B) Plot of mole fraction $Cu_{0.526}Fe_{0.526}Se$ in chalcopyrite vs mole fraction PbSe in galena. Size of circles is approximately 2 times analytical uncertainty. Lines illustrating two different models for the distribution coefficient are shown in both diagrams. Solid line drawn for reduced distribution coefficient $(K' = PbSe/Cu_{0.526}Fe_{0.526}Se = 12.0)$; dashed line drawn for true distribution coefficient $(K = PbSe \cdot Cu_{0.526}Fe_{0.526}S/PbS \cdot Cu_{0.526}Fe_{0.526}Se)$. Upper portion of curve for true distribution constant in (B) is metastable. $Cu_{0.526}Fe_{0.526}S - Cu_{0.526}Fe_{0.526}Se$ becomes nonbinary at compositions somewhere above 36.8 mole percent $Cu_{0.526}Fe_{0.526}Se$. Composition of breakdown point not determined.

range of compositions investigated. Because K' should $\rightarrow K$ as Se $\rightarrow 0$ we have drawn the two relationships tangent at 0 selenium content in Figure 8A. However, we lack an appreciable composition range over which we can demonstrate that $K \approx K'$, and thus we have no reason to assume that the constants we derived are applicable to the much more dilute composition found in most ores.

In the preceding system our confidence in the extrapolation of the reported distribution coefficients is based on the apparently ideal behavior of PbS-PbSe and ZnS-ZnSe solid solutions throughout the temperature and composition range investigated. In the systems describing the distribution of cadmium and manganese between sphalerite and galena the extrapolation was based on the consistency of our data with an assumption of Henry's law behavior. In the present system, however, the behavior of the chalcopyrite-eskebornite solid solutions is demonstrably nonideal; nor does it fit a regular solution model. Further, our data, although they may approach it, do not demonstrate Henry's law behavior. Without a thermodynamic basis, we cannot be confident of any extrapolation of our data to lower concentration ranges.

Second, the well-known nonstoichiometry of chalcopyrite at high temperatures forced us to choose an arbitrary metal rich composition ($CuFeS_{1.92}$) for a phase known to vary widely in composition. Natural chalcopyrites can have a wide range of compositions at high temperatures (e.g., 600° C) but cluster near ideal $CuFeS_2$ at low temperatures.[9] The magnitude of the influence of this compositional variation on the fractionation of sulfur and selenium between chalcopyrite and galena is unknown.

Third, the ability of the system to equilibrate in 72 days at only 390° C implies that natural chalcopyrite-galena pairs are highly susceptible to retrograde reactions following deposition. Problems of postdepositional changes are discussed in a following section.

Distribution of Selenium between Chalcopyrite and Sphalerite

No experiments were performed on the distribution of selenium between chalcopyrite and sphalerite. However, the equation for the variation of

[9] An additional complication is the inversion in the 500°–600° C region from the cubic high temperature form to the tetragonal form stable at lower temperatures.
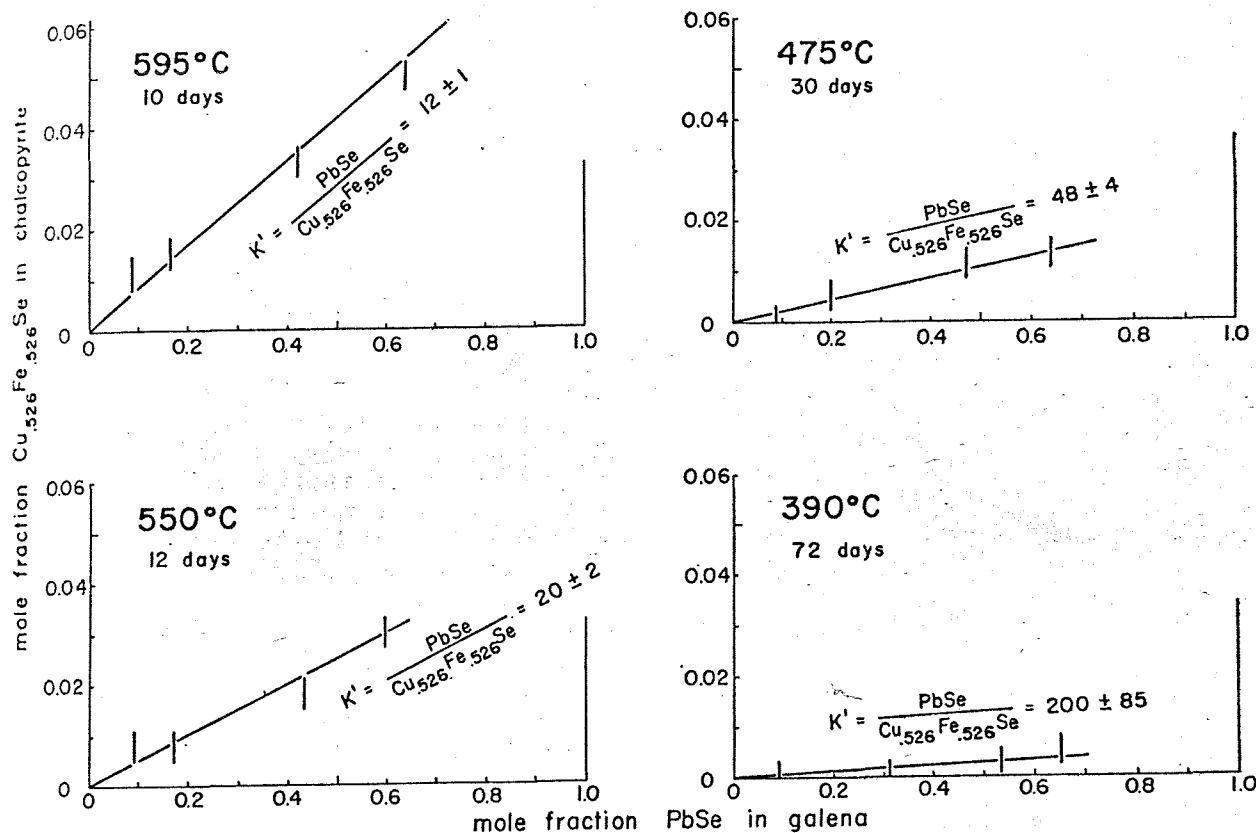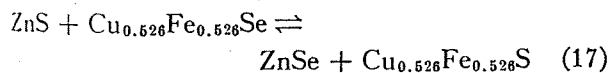
FIG. 9. Mole fraction $Cu_{0.526}Fe_{0.526}Se$ in chalcopyrite vs mole fraction PbSe in galena. Experimental data for 4 temperatures. Construction and notation as in Figure 8B. Note short duration of runs.

the distribution constant with temperature for the reaction:

$$ZnS + Cu_{0.526}Fe_{0.526}Se \rightleftharpoons$$
$$ZnSe + Cu_{0.526}Fe_{0.526}S \quad (17)$$

can be calculated by algebraic combination of the equations describing the distribution of selenium between galena and sphalerite and between galena and chalcopyrite. Such calculations indicate that selenium is moderately fractionated toward chalcopyrite in the expected temperature range of ore deposits, and that, in contrast to the other systems studied, the degree of fractionation *decreases* with decreasing temperature. We may also note that the slope of the curve so calculated is very low, precluding its use in geothermometry.

Rates of Reaction

Although our experiments were not designed to provide quantitative information on reaction rates, we wish to call attention to the vastly different times required for equilibrium between galena-chalcopyrite pairs (10 days at 595° C) as opposed o galena-sphalerite pairs (210–230 days at 600° C).

It is readily apparent that the limiting factor is the equilibration of the sphalerite, and that galena is capable of reacting at least two orders of magnitude faster than sphalerite at 600° C, and presumably at lower temperatures as well. Studies in the PbS-PbTe system by us (unpublished) and Darrow, White and Roy (1966) indicate even faster reaction rates for galena-based solid solutions. The importance of these observations is that they indicate that the upper temperature limit of application of our data to natural assemblages will be strongly influenced by the ability of galena to retain its original composition during postdepositional cooling.

Combination with Fluid Inclusion Thermometry

The small effect of pressure on the distribution coefficients for the systems studied permits the combination of minor element distribution and fluid inclusion geothermometry where significant pressure corrections often must be made. The application is illustrated schematically in Figure 12. In this illustration the P-V-T relations of an aqueous solution containing 10% NaCl calculated from the data of Klevtsov and Lemmlein (1959) are superimposed on the P-T curves for the dis-

A

$$\text{Log } K_{Se}^{gn:sp} = (2,850/T^{\circ}_{K}) - 1.24$$

B

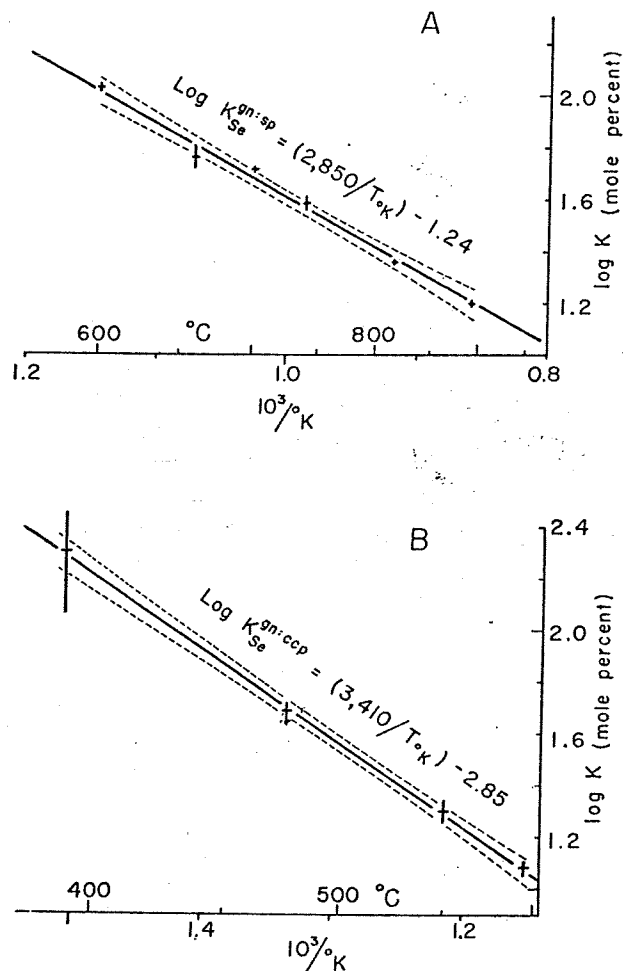$$\text{Log } K_{Se}^{gn:ccp} = (3,410/T^{\circ}_{K}) - 2.85$$

FIG. 10. Variation of distribution coefficients with temperature. (A) Distribution of selenium between galena and sphalerite. (B) Distribution of selenium between galena and chalcopyrite (reduced distribution coefficient shown). Size of crosses indicates uncertainty in estimation of distribution coefficients and $\pm 5^{\circ}$ C in temperature. 90 percent confidence interval indicated by dashed lines.

tribution of manganese between sphalerite and galena calculated from our data. It is assumed that a filling temperature (T_H) of $250^{\circ} \pm 10^{\circ}$ C has been determined from a group of contemporaneous fluid inclusions in sphalerite and that the composition of the fluid has been determined to be that chosen for the illustration. The distribution of manganese between the sphalerite and a contemporaneous galena yields a temperature (T_D) of $400 \pm 20^{\circ}$ C. The intersection of these two curves provides a corrected temperature-pressure estimate of 385° C and 1,500 bars $\pm 20^{\circ}$ C and ± 300 bars. Obviously, the combination of the two methods yields considerably more information than either of the two applied separately.

Problems of Application

Within the limitations specified, our experimental studies provide a basis for the estimation of temperatures of ore deposition. However, the problems of actual application are imposing, and the utility of the approach remains to be demonstrated. In the paragraphs below we will briefly discuss only some of the more obvious of these problems.

Analytical and Sampling Restrictions

The strong fractionation in the systems we have studied presents considerable difficulty in the sampling and chemical analysis of the minerals involved. Concentrations of the minor elements will be very low in the impoverished phase under most conceivable environments. Highly sensitive and precise analytical techniques are required in most instances, and since we are dealing with vastly different concentration ranges in two different matrices, opportunities for systematic errors to creep into the analyses are plentiful. The strong fractionation further requires a nearly absolute degree of sample purity, for even minute amounts of the enriched phase may add significant amounts of the minor element to the analysis of the depleted phase. The magnitude of this effect is illustrated in Figure 13 where an apparent temperature of formation has been calculated as a function of the weight percent impurity of the enriched phase in the impoverished phase for a mineral pair equilibrated at 300° C. This effect can be corrected if the contents of zinc and lead are determined in the galena and sphalerite concentrates, respectively, assuming that both metals are present only as physical impurities of sphalerite or galena.

Paragenetic Restrictions

The premier requirement for the successful application of minor element distribution is that the mineral pair must have been in equilibrium at the time of emplacement, and that postdepositional changes have not altered the compositions of the phases. Failure of an assemblage to meet these requirements will lead at best to an indecipherable scatter of data, and at worst to a misleading, but apparently consistent, relationship. Barton, Bethke and Toulmin (1963) have discussed the general problem of equilibrium in ore deposits in some detail, but several ramifications of arguments presented therein have particular significance to the distribution of minor elements.

Depositional Phenomena.—Deposition of a mineral pair in mutual equilibrium implies that both crystals were in equilibrium with the ore fluid. Because of the relatively rapid reaction rates
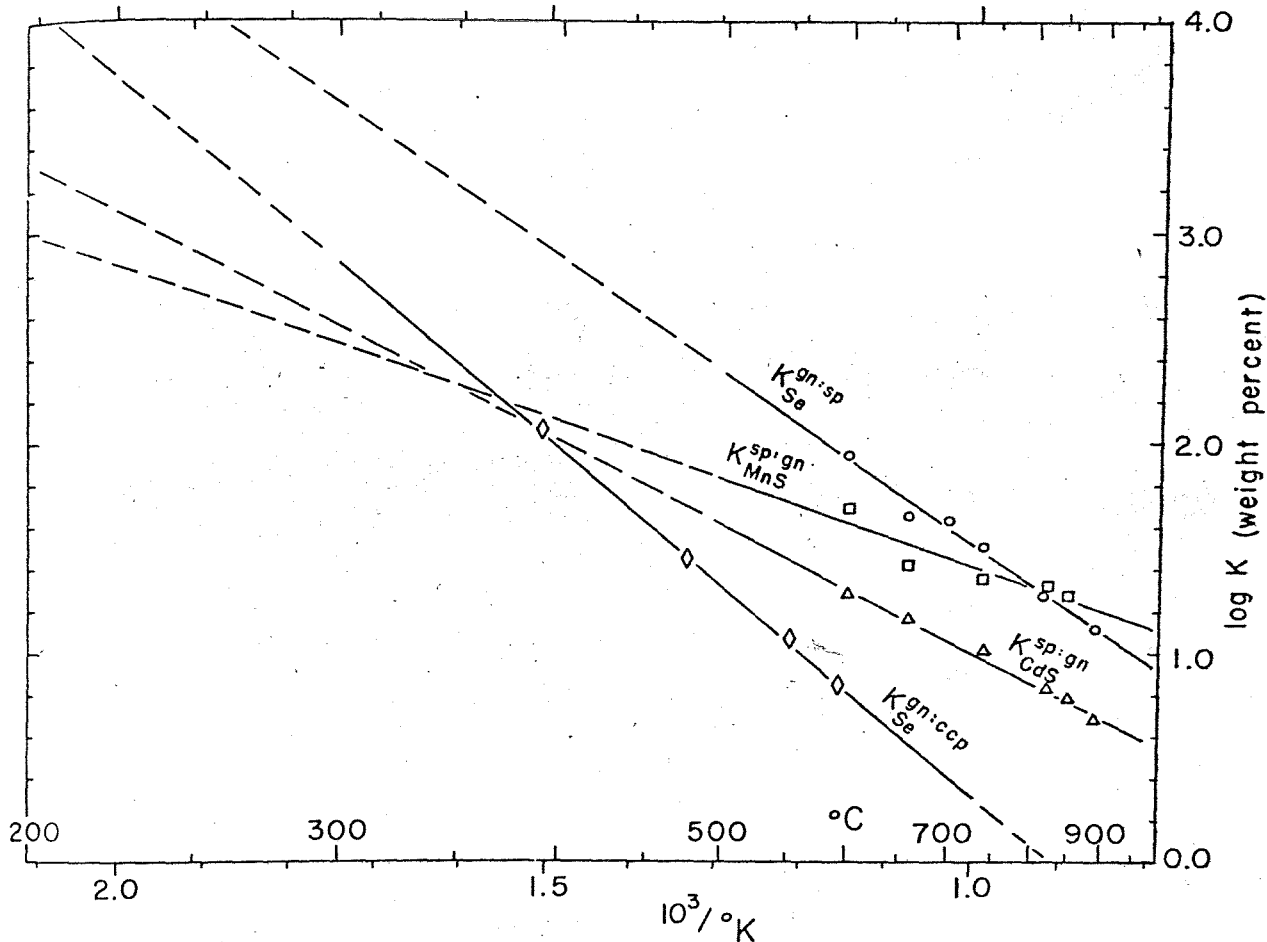
FIG. 11. Summary of variation of distribution coefficients with temperature. Mole fraction values converted to weight percent basis. (Reduced distribution coefficient shown for distribution of selenium between chalcopyrite and galena.)

between crystals and the solutions from which they have grown, we may be somewhat optimistic about finding mineral pairs grown in equilibrium, although non-equilibrium deposition is far from rare (Barton, Bethke and Toulmin, 1963). The activity of many minor components in the ore fluid may fluctuate by several orders of magnitude in response to changes in the chemical environment (see discussion by Barton, 1970). If equilibrium crystallization proceeded under such fluctuating conditions, the geometrically simplest result would be growth zoning in single crystals or banding in polycrystalline aggregates in simple vein fillings. Providing that solid state diffusion was sufficiently sluggish to prevent the crystals from equilibrating internally, the zoned crystals produced would represent a series of superimposed equilibria of widely varying compositions, or in the terminology of Thompson (1959), a set of local equilibria. In massive or replacement bodies the geometric relations of these domains representing

local equilibrium might be much more complex. It should be obvious that such compositional heterogeneity must be recognized in the mineral assemblage, and that only samples taken from contemporaneous zones can yield valid results. In many assemblages it will be difficult or impossible to obtain sufficient amounts of valid samples to provide accurate analyses. Without attempting a complete discussion, we might point out that marked heterogeneity in both the manganese and selenium content of ore minerals appears to be very common, whereas the distribution of cadmium tends to be far more uniform.

Postdepositional Phenomena.—The thermal history of many ore deposits may have been such that postdepositional changes have obscured the original record. The relatively high diffusion rates in galena and chalcopyrite make these phases particularly suspect. Let us consider the simultaneous deposition of a sphalerite-galena pair. If the temperature of emplacement is high enough, an entire
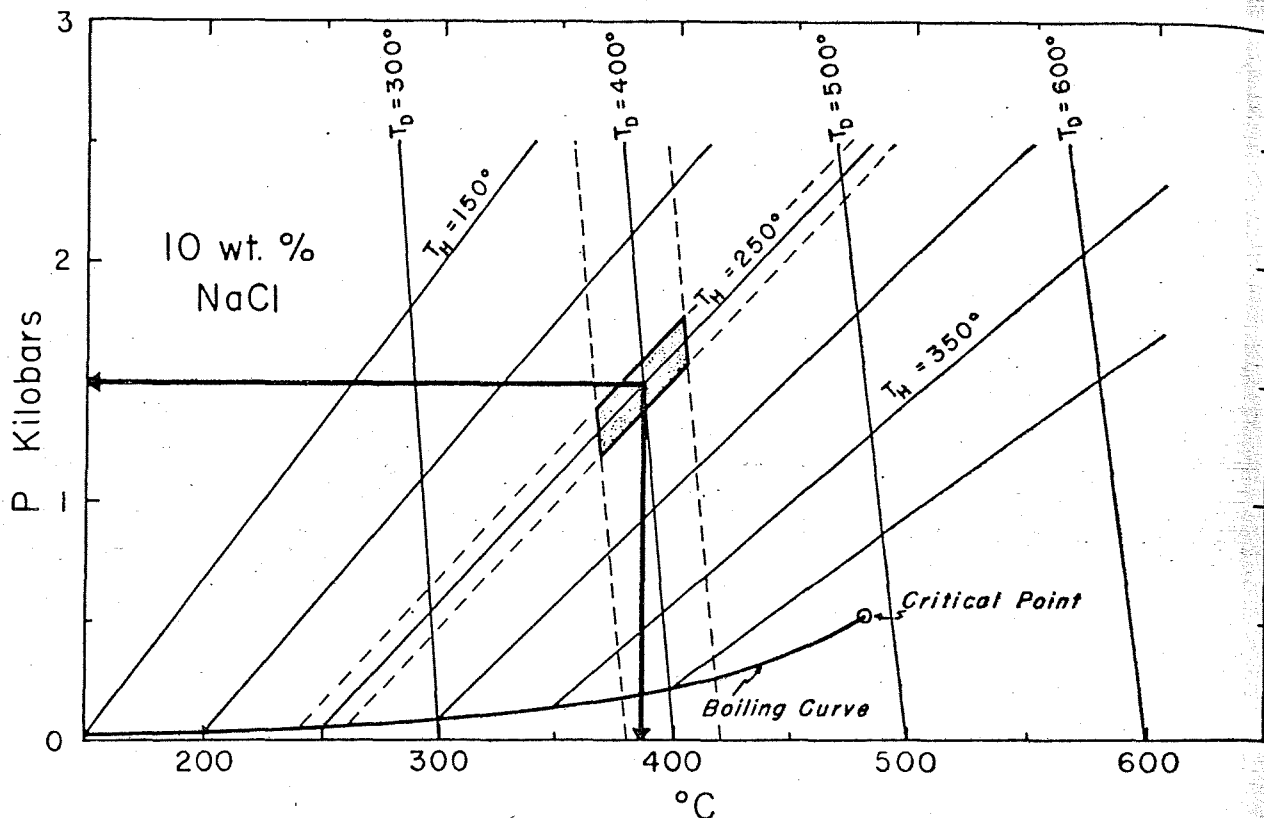
FIG. 12. Superposition of P-V-T data for 10 weight percent NaCl brine on P-T relations for the distribution of manganese between sphalerite and galena, illustrating method of estimating both temperature and pressure of deposition by combining minor element distribution and fluid inclusion thermometry. T_H = temperature of homogenization of fluid inclusion; T_D = temperature of formation computed from distribution of MnS between sphalerite and galena. Dashed lines represent reasonable uncertainties in estimation of apparent temperatures. Stippled area is region of uncertainty in the resulting P-T estimate.

galena crystal may be able to maintain itself in equilibrium with the ore fluid therefore not preserving any record of compositional fluctuations, while its neighboring sphalerite crystal, in which diffusion rates are much lower, may record such fluctuations in minute detail. At somewhat lower temperatures of formation, diffusion rates in the galena may be slow enough, relative to rates of crystal growth, to establish growth zoning, but such zoning may be gradually erased if deposition is followed by very slow cooling.

In addition to re-equilibration within galena crystals themselves, we must also consider post-depositional reaction between adjacent galena and sphalerite grains. As the value of the distribution coefficient increases during cooling neighboring sphalerite and galena grains will attempt to maintain equilibrium concentrations by transfer of CdS and MnS out of the galena into the sphalerite or by exchange of selenium and sulfur between galena and sphalerite. If the rate of such reaction is fast enough, relative to the rate of cooling, significant alteration of the original state may occur.

The rate controlling process in this case will be the solid state diffusion of material into and out of the sphalerite. The times required for equilibration in our experimental runs indicate that considerable reaction may take place in the upper temperature ranges generally assumed for ore deposition. In high temperature ore deposits, or those subject to high grade metamorphism, equilibration may be essentially complete near the peak of the thermal history, but as the deposit cools, diffusion in the sphalerite will eventually become so attenuated that only the edges of grains adjacent to the galena will be involved, and reaction rims, slightly enriched in manganese and cadmium and very much depleted in selenium will develop. Assemblages formed at, or subjected to, moderate temperatures might be expected to show only reaction rims.

As we have previously noted (Bethke and Barton, 1959) perhaps the best test for the attainment and preservation of equilibrium compositions between the phases will be provided by the distribution data themselves, for concordant temperature
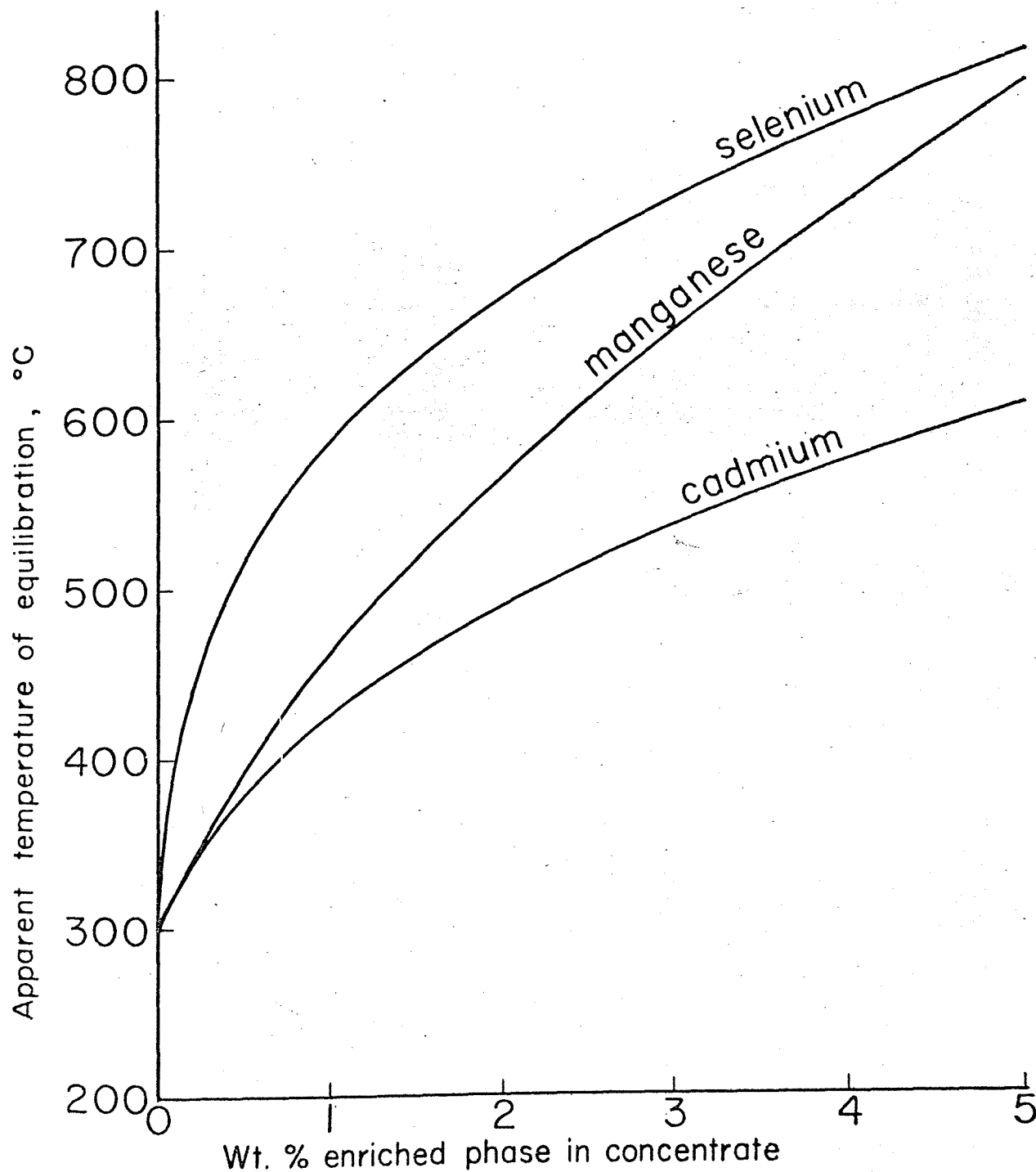
FIG. 13. Diagram indicating magnitude of errors due to contamination of concentrate of impoverished phase by small amounts of enriched phase. Calculated for the distribution of selenium, manganese and cadmium for a sphalerite-galena pair assumed to have equilibrated at 300° C.

estimates should be obtained for all of the elements determined.

The conceivable difficulties in the application of the results of this study to real ores are legion and cannot possibly be summarized here. Each mineral assemblage will contain its own set of complications with which the investigator will have to deal. We feel that the limitations on the method may be

severe and may greatly restrict the number of ore deposits to which the method can be successfully applied.

If we have seemed to overemphasize the inherent difficulties in the use of the distribution of minor elements between coexisting minerals, it is, perhaps, due to our own experience that the successful application of laboratory studies to natural assemblages requires considerably more effort and good fortune than does the pursuit of the experimental work itself.

Summary

We may briefly summarize the conclusions drawn from our studies as follows:

1. Under equilibrium conditions cadmium and manganese are strongly fractionated toward sphalerite (or wurtzite) relative to galena in the temperature range of ore deposition, the fractionation becoming stronger with decreasing temperature.

2. At temperatures below 800° C selenium is fractionated under equilibrium conditions according to the following sequence of increasing selenium content: sphalerite-chalcopyrite-galena. The fractionation between galena and sphalerite and galena and chalcopyrite becomes stronger with decreasing temperature, and that between chalcopyrite and sphalerite stronger with increasing temperature.

3. Cadmium- and manganese-bearing galena and sphalerite solid solutions appear to exhibit Henry's law behavior well beyond geologically reasonable concentration ranges. Selenium-bearing galena and sphalerite solid solutions behave sensibly as ideal solid solutions above 600° C. Thus, the distribution of cadmium, manganese and selenium between sphalerite and galena in natural assemblages may be treated as functions of temperature and pressure alone, and, our experimental results, most of which were gathered at significantly higher concentrations than expected in natural assemblages, are applicable to mineral pairs containing only trace amounts of the distributed component.

4. The variation of the distribution coefficient with temperature is large enough in each of the above systems to permit temperature estimates to a precision of 15°–20° C, assuming normal precision in the analyses of naturally occurring mineral pairs.

5. The effect of pressure on the distribution coefficients, as calculated from molar volume data, is too small to be of significance in the estimation of temperatures of formation, and, in fact, is so small that for most purposes it can be neglected.

6. Assuming a linear extrapolation of our data to low temperatures, the magnitude of the distribution coefficients is low enough in the temperature range of ore deposition to permit precise temperature estimates for many deposits formed as low as 200° C.

7. Extrapolation of our data to lower temperatures remains tenuous, and it is necessary to determine the values of the various distribution constants in the range 200°–500° C.

8. Polytyping of natural sphalerites, if unrecognized, may lead to considerable under-estimation of temperature of formation. Rough corrections can probably be applied if the proportions of the sphalerite and wurtzite "layers" can be determined.

9. Solid state reaction rates in galena are high enough that re-equilibration following deposition may be common, particularly in higher temperature deposits.

10. The distribution of selenium between chalcopyrite and galena appears promising, but we cannot show that our results may be applied to the lower selenium contents expected in ores, and the potential usefulness is complicated by compositional variation in chalcopyrite and the strong possibility of retrograde reaction down to very low temperatures.

11. The distribution of selenium between chalcopyrite and sphalerite is relatively insensitive to both temperature and pressure and therefore does not present sufficient precision to be useful as a geothermometer.

12. By utilizing the distribution of minor elements in conjunction with the filling temperatures of fluid inclusions both temperature and pressure of ore deposition may be estimated.

13. The concentration of cadmium, manganese and selenium in the impoverished phase should be very low in most ore deposits thereby requiring a nearly absolute degree of sample purity and the use of highly sensitive analytical techniques.

14. Successful application of the method requires the recognition of a region of apparent local equilibrium of sufficient size to permit adequate sampling and the demonstration that equilibrium did obtain and was frozen in.

15. The problems of application of the method are imposing and may greatly restrict the number of ore deposits to which it may be successfully applied.

grateful to our colleague, Priestley Toulmin, III, for continued discussion and helpful criticism.

REFERENCES

Barton, P. B., Jr., 1970, Sulfide petrology: Mineral. Soc. Am. Special Paper 3, p. 187–198.

——, Bethke, P. M., and Toulmin, P., III, 1963, Equilibrium in ore deposits: Mineral. Soc. Am. Special Paper 1, p. 171–185.

——, and Skinner, B. J., 1967, Sulfide mineral stabilities, *in* Geochemistry of Hydrothermal Ore Deposits, H. L. Barnes, editor: New York, Holt, Rinehart and Winston, p. 236–333.

Bethke, P. M., 1961, Unit-cell dimensions versus composition in the systems: PbS-CdS, PbS-PbSe, ZnS-ZnSe, and $CuFeS_{1.90}$-$CuFeSe_{1.90}$: U. S. Geol. Survey Prof. Paper 424-B, p. 266–270.

——, and Barton, P. B., Jr., 1959, Trace element distribution as an indicator of temperature and pressure of ore deposition (abs.): Geol. Soc. America, Bull. v. 70, p. 1569–1570.

——, and Page, N. J., 1958, Preliminary experiments on the distribution of selenium between co-existing sulfides (abs.): Geol. Soc. America, Bull. v. 69, p. 1759–1760.

Darrow, M. S., White, W. B., and Roy, R., 1966, Phase relations in the system PbS-PbTe: Trans. Metall. Soc. of AIME, v. 236, p. 654–658.

Friedman, I., 1949, A proposed method for the measurement of geologic temperatures: J. Geol., v. 57, p. 618–619.

Guggenheim, E. A., 1950, Thermodynamics, Second Edition: Amsterdam, North-Holland Publishing Company, 412 p.

Halbig, Joseph B., 1969, Trace element studies in synthetic sulfide systems: The solubility of thallium in sphalerite and the partition of selenium between sphalerite and galena: Ph.D. Dissertation, College of Earth and Mineral Sciences, The Pennsylvania State University.

Holland, H. D., 1956, The chemical composition of vein minerals and the nature of ore forming fluids: Econ Geol., v. 51, p. 781–797.

Hurlbut, C. S., Jr., 1957, The wurtzite-greenockite series: Am. Min., v. 42, p. 184–190.

Juza, R., Rabenau A., and Pascher, G., 1956, Über feste lösungen in den systemen ZnS/MnS, ZnSe/MnSe, ZnTe/MnTe: Zeit. anorg. und allgem. Chemie, v. 285, p. 61–69.

Klevtsov, P. V., and Lemmlein, G. G., 1959, Pressure corrections for the homogenization of aqueous NaCl solutions: Akad. Nauk. SSSR, Doklady, v. 128, no. 6, p. 1250–1253, in Russian; (Translated in Amer. Geol. Inst. Doklady of the Acad of Sciences of the USSR, v. 128, nos. 1–6, p. 995–997 (1960))

Kretz, R., 1959, Chemical Study of garnet, biotite, and hornblende from gneisses of southwestern Quebec, with emphasis on distribution of elements in coexisting minerals: J. Geol., v. 67, p. 371–402.

——, 1960, The distribution of certain elements among coexisting calcic pyroxenes, calcic amphiboles and biotites in skarns: Geochim. et Cosmochim. Acta, v. 20, p. 161–191.

——, 1961, Some applications of thermodynamics to coexisting minerals of variable composition. Example: orthopyroxene-clinopyroxene and orthopyroxene-garnet: J. Geol., v. 69, p. 361–387.

Kroger, F. A., 1938, Formation of solid solutions in the system zinc sulfide-manganese sulfide: Zeit. Krist. A100, p. 543–545.

——, 1939, Solid solutions in the ternary system ZnS-CdS-MnS: Zeit. Krist., A102, p. 132–135.

Kubaschewski, O., Evans, E. Ll., and Alcock, C. B., 1967, Metallurgical Thermochemistry, 4th Ed.: New York, Pergamon Press, 495 p.

Kullerud, G., 1953, The FeS-ZnS system, a geothermometer: Norsk. Geol. Tidsskr., v. 32, p. 61–147.

McIntire, W. L., 1963, Trace element partition coefficients—a review of theory and applications to geology: Geochim. et Cosmochim. Acta, v. 27, p. 1209–1264.

Robie, R. A., Bethke, P. M., and Beardsley, K. M., 1967, Selected x-ray crystallographic data, molar volumes and densities of minerals and related substances: U. S. Geol. Survey Bull. 1248, 87 p.

Sims, P. K., and Barton, P. B., Jr., 1961, Some aspects of the geochemistry of sphalerite, Central City district, Colorado: Econ. Geol., v. 56, p. 1211–1237.

Skinner, B. J., 1961, Unit-cell edges of natural and synthetic sphalerites: Am. Min., v. 46, p. 1399–1411.

——, 1962, Thermal expansion of ten minerals: Art. 152, U. S. Geol. Survey Prof. Paper 450D, p. 109–112.

——, and Bethke, P. M., 1961, The relationship between unit-cell edges and compositions of synthetic wurtzites: Am. Min., v. 46, p. 1382–1398.

Thompson, J. B., 1959, Local equilibrium in metasomatic processes: *in* Researches in Geochemistry, P. H. Abelson, editor: New York, John Wiley and Sons, p. 427–457.

Tischendorf, G., 1960, Über Eskebornit von Tilkerode im Harz: Neues Jahrb. Mineral. Abh., v. 94, p. 1169–1182.

Van Hook, H. J., 1960, The ternary system Ag_2S-Bi_2S_3-PbS: Econ. Geol. v. 55, p. 759–788.